

Next steps in wind tunnel aeroacoustics: Measurements at flight-Reynolds numbers

Thomas Ahlefeldt

German Aerospace Center (DLR), Institute of Aerodynamics and Flow Technology,
Experimental Methods, 37073 Göttingen, Germany

A large, curved image of the Earth from space occupies the bottom right portion of the slide. It shows a view of the Earth's surface with blue oceans, green landmasses, and white clouds. The curvature of the planet is clearly visible, creating a sense of depth and global perspective.

Knowledge for Tomorrow

Acknowledgments

Aeroacoustic Measurement Technique Group Göttingen

- Measurements in WT and flight tests
- (Dr. Lars Koop), Dr. Carsten Spehr, Dr. Thomas Ahlefeldt, Dr. Stefan Haxter, Daniel Ernst, Hans-Georg Raumer



Federal Ministry of Economics and Technology

- Financial support



European Transonic Windtunnel

- Provided Infrastructure
- Jürgen Quest: project leader



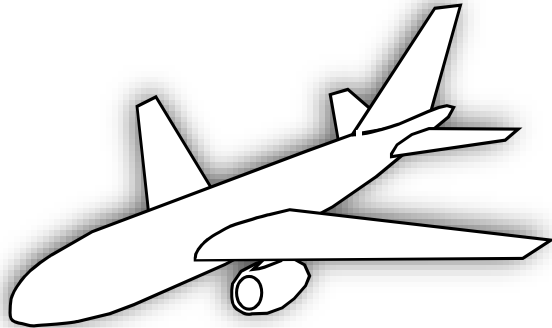
Airbus

- Provision of the model
- Iris Goldhahn: cooperation



Background

Original



$Re \approx 20 \text{ Mio}$



Scaled model in Wind Tunnel



standard

$Re \approx 1.4 \text{ Mio}$



cryogenic or
pressurized

$Re \approx 5.2 \text{ Mio}$



cryogenic and
pressurized

$Re \approx 20 \text{ Mio}$



- Model fidelity
- Installation effects
- Reynolds number, Mach number, Strouhal number



Previous work

Aeroacoustic measurements in wind tunnels

Hayes [1999] at NTF

- Pressurized environment

Stoker [2008] at NTF

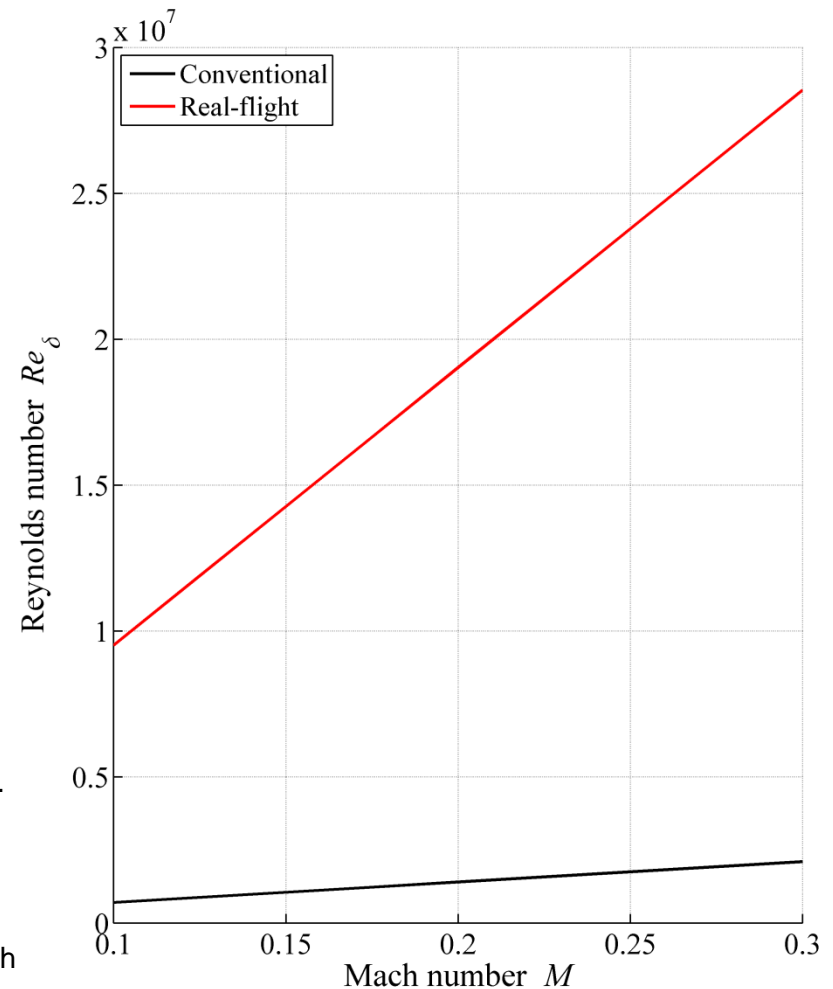
- Pressurized and mild cryogenic ($T = 226.5 \text{ K}$)

Ahlefeldt [2010] at DNW-KKK

- Cryogenic ($T = 100 \text{ K}$)

- [1] Hayes, J. A. et. al., „Measurement of Reynolds number effects on airframe noise in the 12-foot pressure wind tunnel”, *5th AIAA/CEAS*, 1999.
- [2] Stoker, R.W. et. al., “High Reynolds Number Aeroacoustic Testing in NASAs National Transonic Facility (NTF)”, *46th AIAA-ASM*, 2008.
- [3] Ahlefeldt T. and Koop L., “Microphone-Array Measurements in a Cryogenic Wind Tunnel”, *AIAA-Journal*, Vol.48, No.7, 2010.
- [4] Ahlefeldt T., “Aeroacoustic Measurements of a Scaled Half Model at High Reynolds Numbers”, *AIAA-Journal*, Vol.51, No.12, 2013.

$$\text{Re} = \frac{\rho \cdot u_{\infty} \cdot d}{\eta} = \frac{\rho \cdot M \cdot d}{c \cdot \eta}$$



Aeroacoustic Measurements at the ETW
Measuring under different conditions (p_{stat}, T)

Beamforming procedure

Experimental setup in ETW

Sensor calibration (p_{stat}, T)

Corrections, Assumptions (p_{stat}, T)

Comparability
(different wind tunnels)

Comparable Results

⇒ Statements on Reynolds number dependency



Aeroacoustic Measurements at the ETW
Measuring under different conditions (p_{stat}, T)

Beamforming procedure

Experimental setup in ETW

Sensor calibration (p_{stat}, T)

Corrections, Assumptions (p_{stat}, T)

Comparability
(different wind tunnels)

Comparable Results

⇒ Statements on Reynolds number dependency



Background: acoustic sources in beamforming

Numerical approach

$$\frac{\partial}{\partial t^2} \rho' - c^2 \Delta \rho' = \frac{\partial^2}{\partial x_i \partial x_j} T_{ij}$$

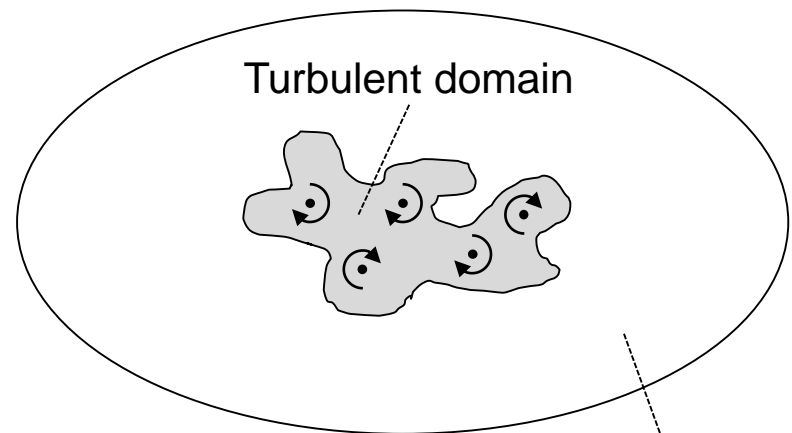
Lighthill equation

⇒ "Equivalent sources"

Application:

$$\rho' = \frac{1}{4\pi c^2} \frac{\partial^2}{\partial x_i \partial x_j} \int_{V_Q} \frac{T_{ij}(\mathbf{y}, t - |\mathbf{x} - \mathbf{y}|/c)}{|\mathbf{x} - \mathbf{y}|} d^3 \mathbf{y}$$

Approximate solution without boundaries



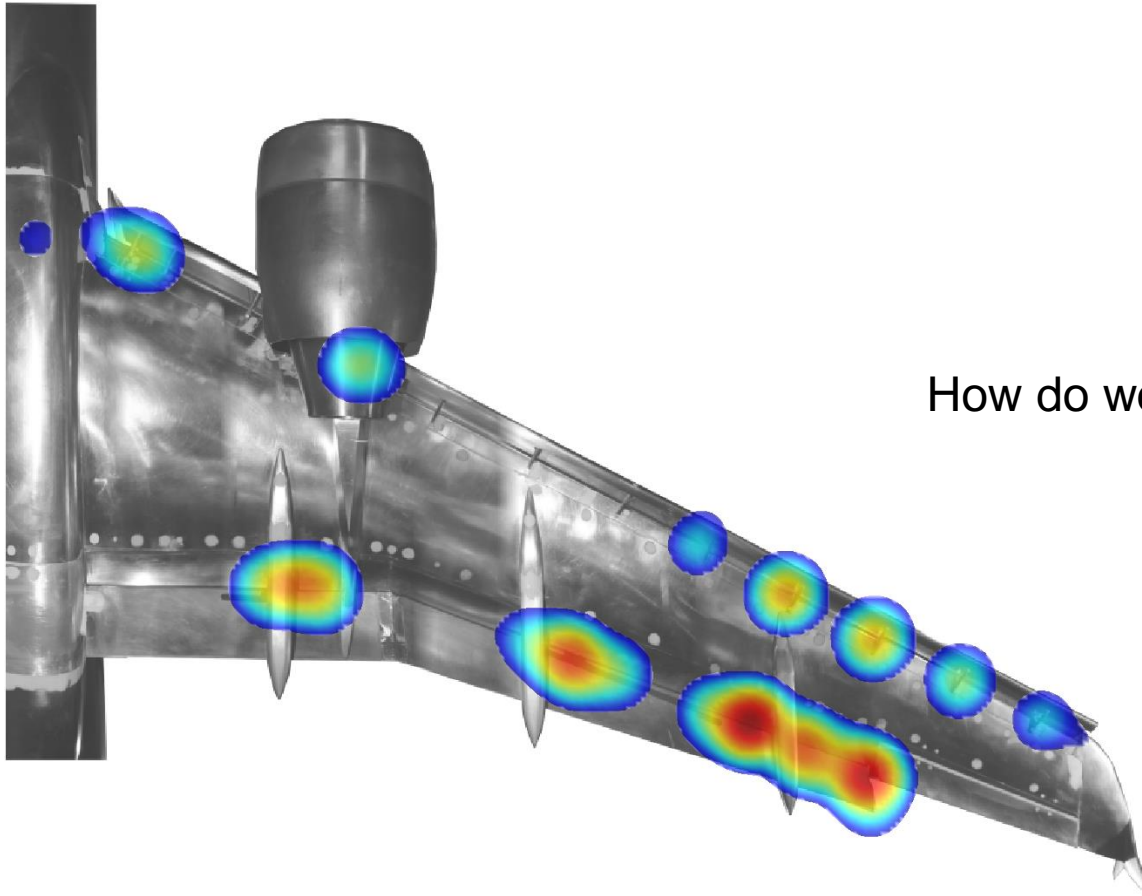
Outside domain:
no flow, $Q = 0$

V_Q : Domain with
non-linear effects



Background: acoustic sources in beamforming

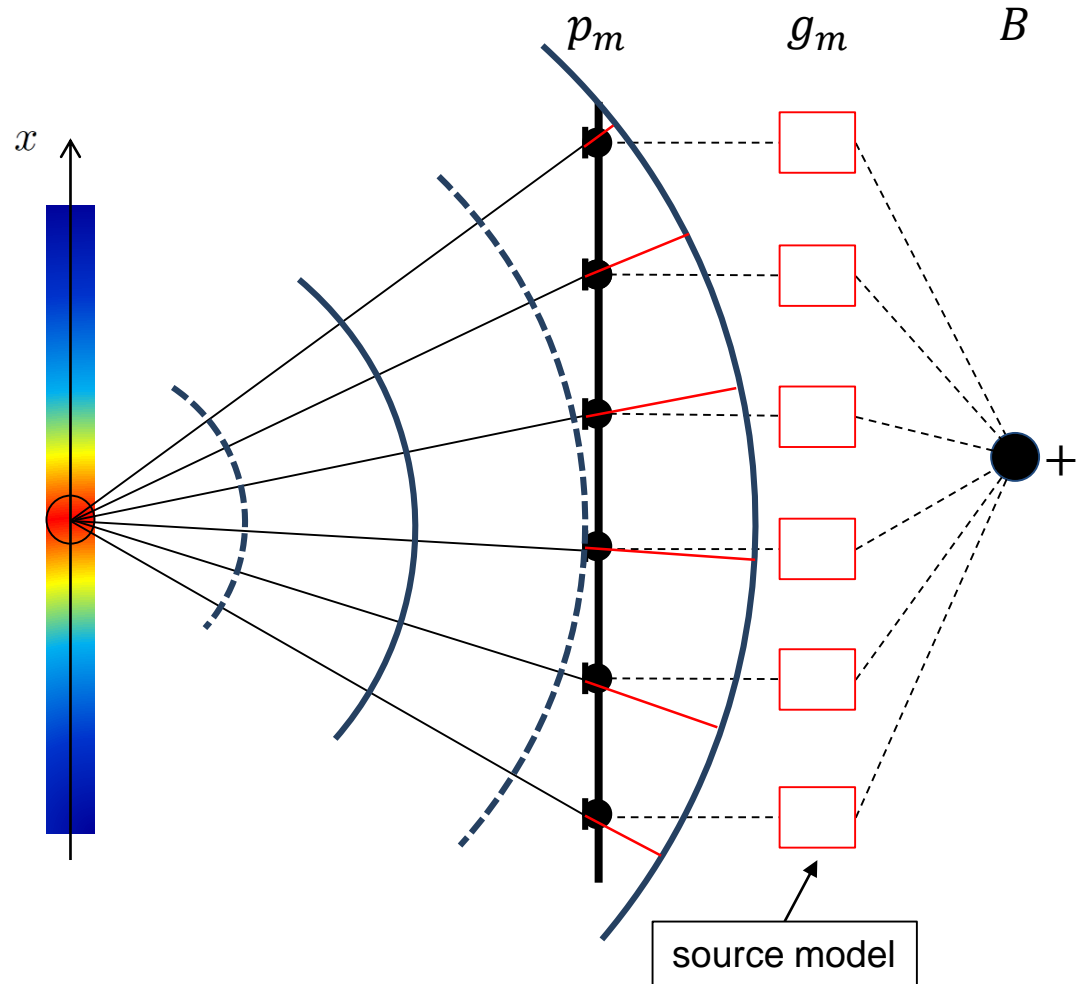
Beamforming approach



Background: acoustic sources in beamforming

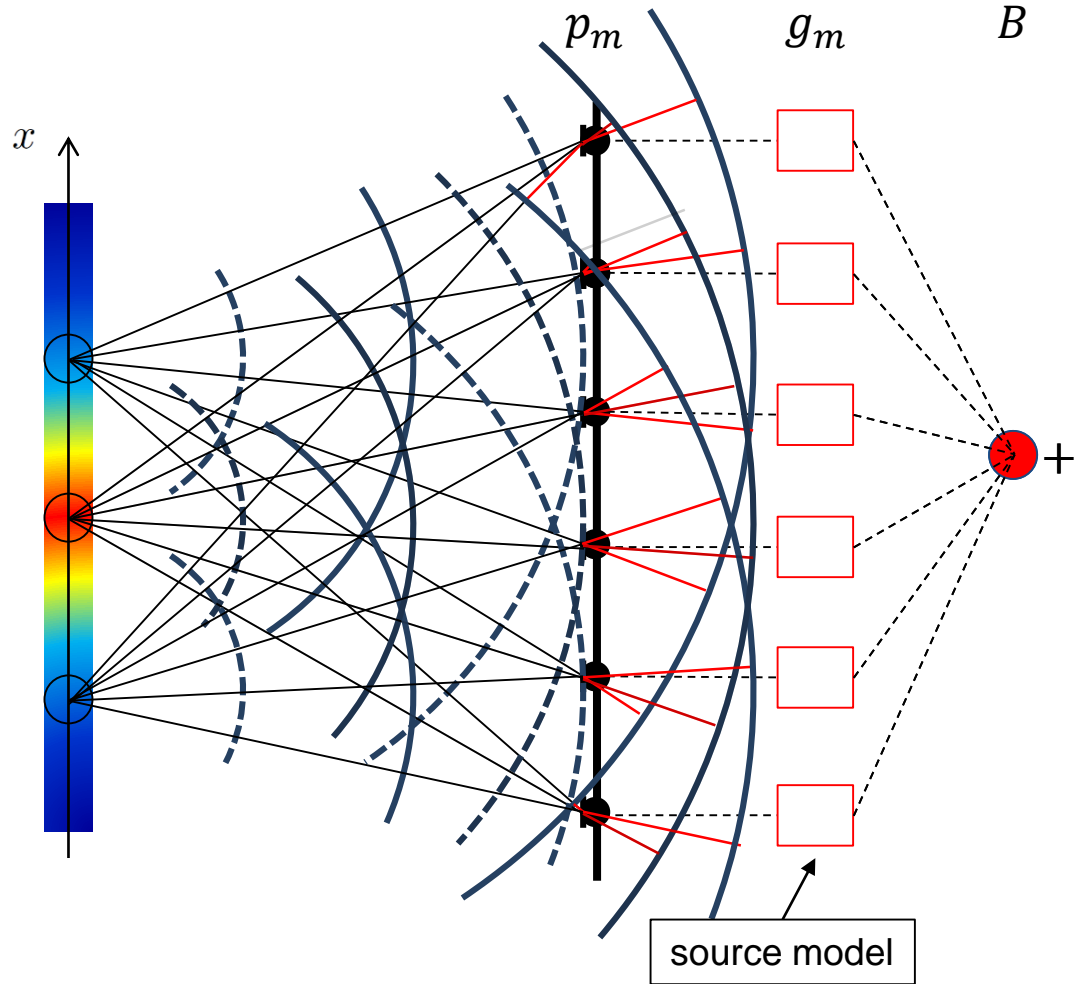
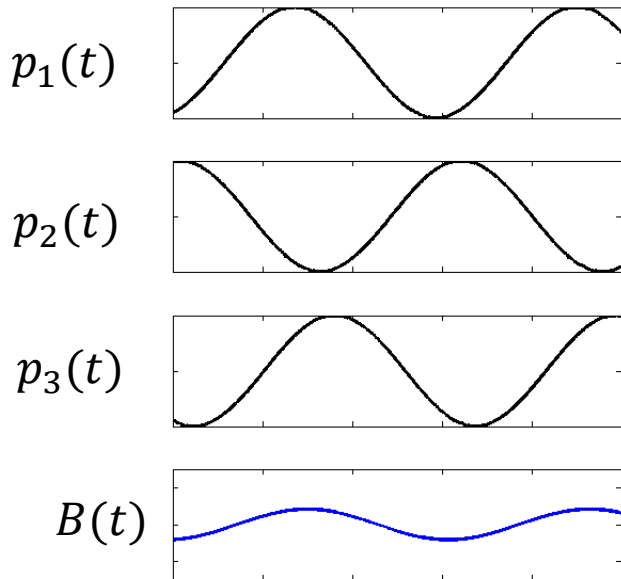
Beamforming approach – time domain

$$B = \sum_{m=1}^M p_m g_m$$



Beamforming approach – time domain

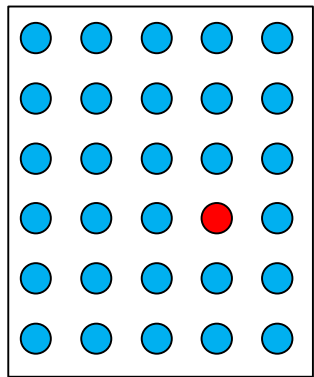
$$B = \sum_{m=1}^M p_m g_m$$



Background: acoustic sources in beamforming

Beamforming approach – frequency domain

Map domain
with focus points y_n ●



Microphones in
far field x_m



Pressure signals and cross spectral matrix
(sampled in time blocks k)

$$\mathbf{p}^{(k)}(\omega) = \begin{pmatrix} p_1^{(k)}(\omega) \\ \vdots \\ p_M^{(k)}(\omega) \end{pmatrix}$$

$$\mathbf{C}(\omega) = \frac{1}{K} \sum_{k=1}^K \mathbf{p}^{(k)}(\omega) \mathbf{p}^{(k)}(\omega)^*$$

Green's function of
convective Helmholtz equation

$$g = \frac{e^{-j\omega\Delta t}}{4\pi\sqrt{(\mathbf{M} \cdot (\mathbf{x} - \mathbf{y}))^2 + \beta^2\|\mathbf{x} - \mathbf{y}\|^2}}$$

$$\text{with } \beta^2 = 1 - \|\mathbf{M}\|^2$$

Steering vector and steering matrix

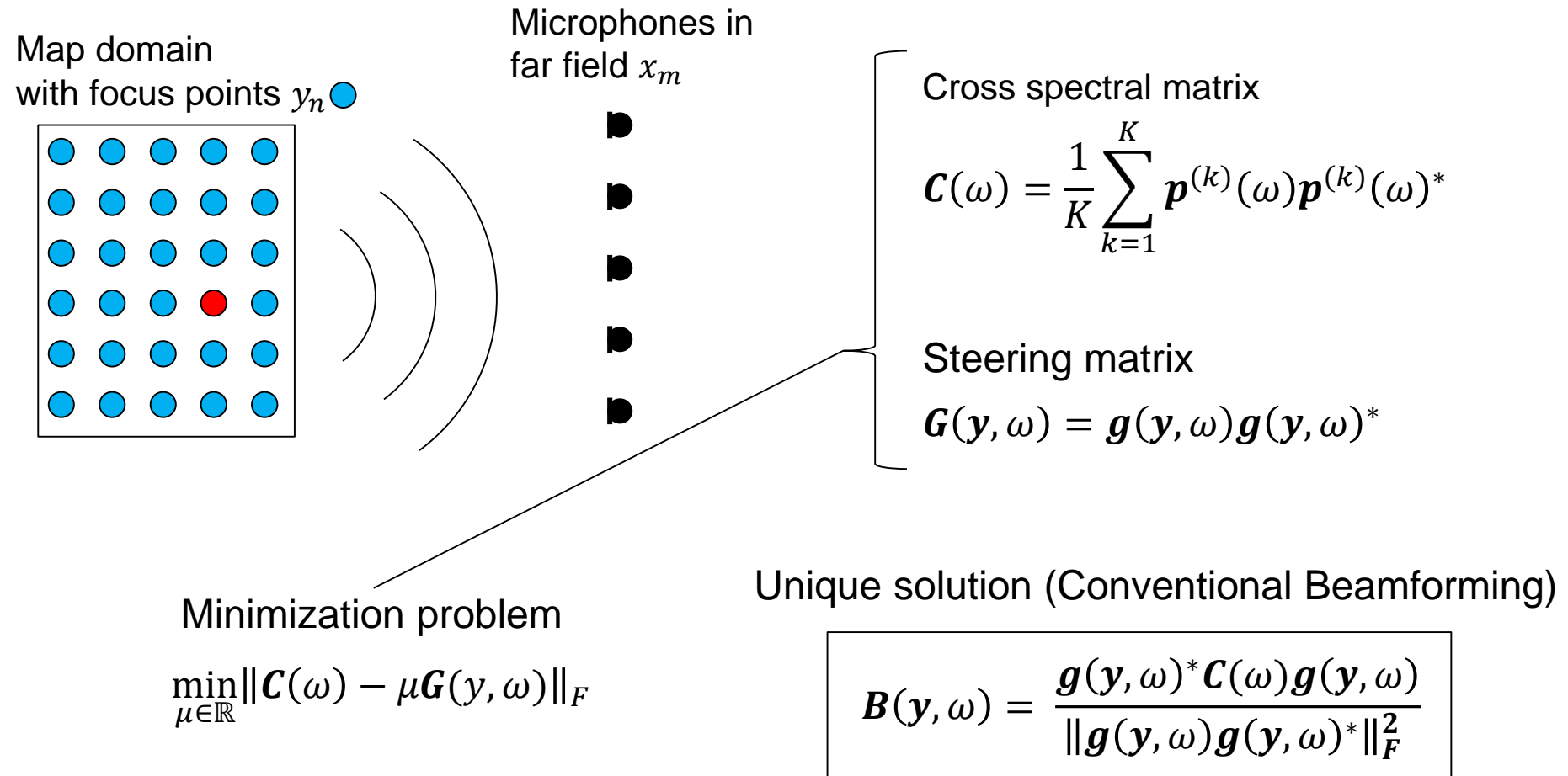
$$\mathbf{g}(\mathbf{y}, \omega) = \begin{pmatrix} g_1(\omega, x_1, \mathbf{y}) \\ \vdots \\ g_M(\omega, x_M, \mathbf{y}) \end{pmatrix}$$

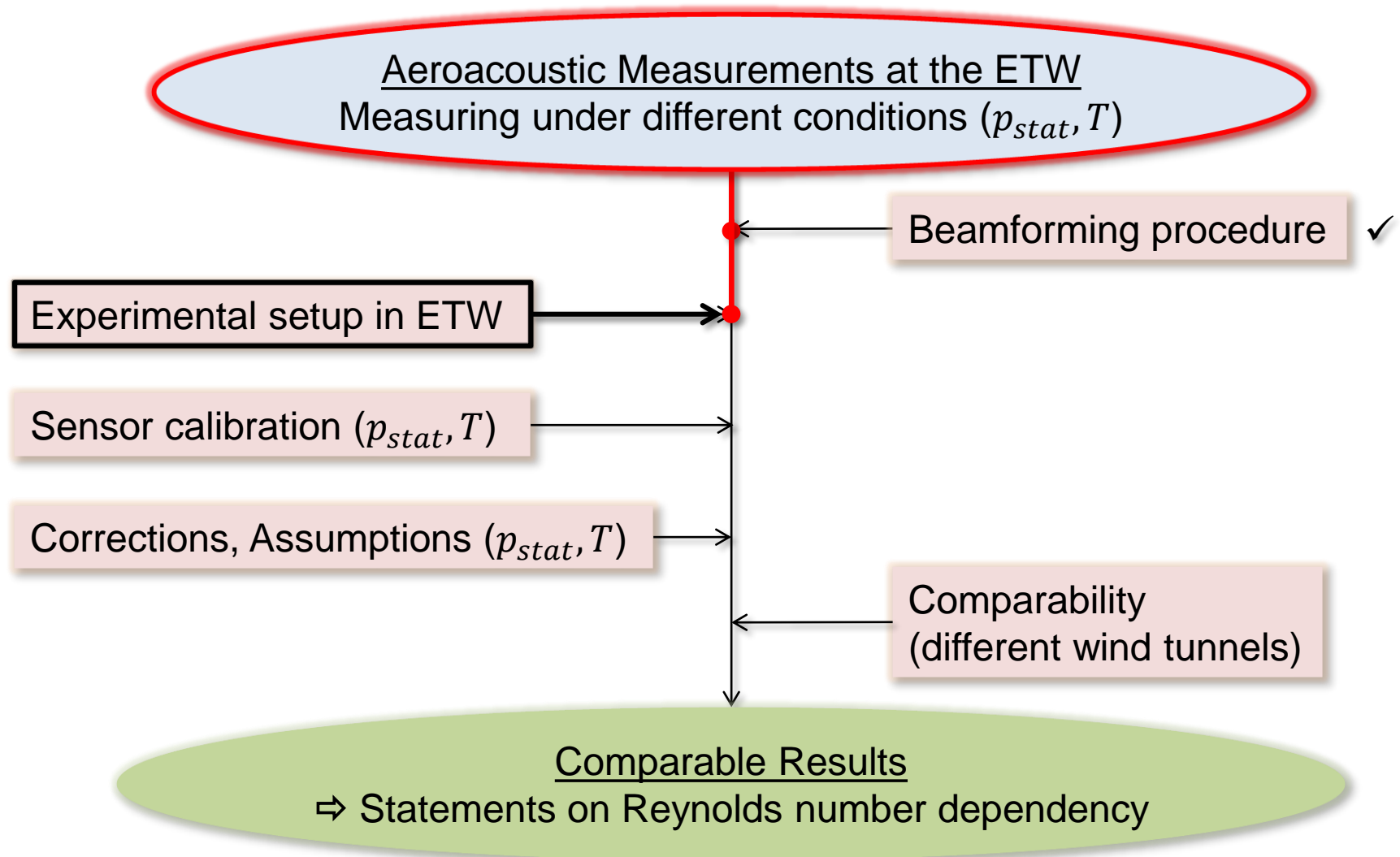
$$\mathbf{G}(\mathbf{y}, \omega) = \mathbf{g}(\mathbf{y}, \omega) \mathbf{g}(\mathbf{y}, \omega)^*$$



Background: acoustic sources in beamforming

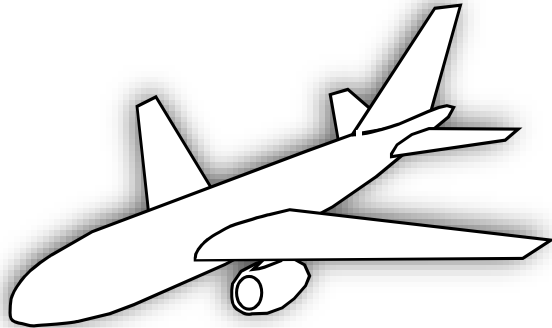
Beamforming approach – frequency domain





Background

Original



$Re \approx 20 \text{ Mio}$



Scaled model in Wind Tunnel



standard

cryogenic or
pressurized

cryogenic and
pressurized

$Re \approx 1.4 \text{ Mio}$

$Re \approx 5.2 \text{ Mio}$

$Re \approx 20 \text{ Mio}$



- Model fidelity
- Installation effects
- Reynolds number, Mach number, Strouhal number



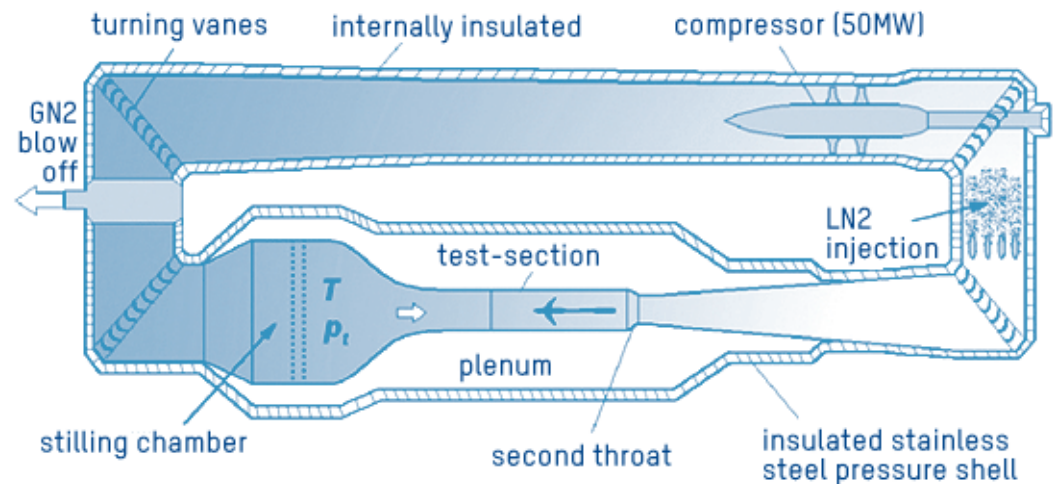
Wind Tunnel

- European Transonic Windtunnel (ETW)
- Provision of real-flight Reynolds numbers by virtue of both decreased temperature and increased pressure
- Test section:
2.0 m × 2.4 m × 9.0 m
- Operational range:

$$0.15 < M < 1.35$$

$$313 \text{ K} > T > 110 \text{ K}$$

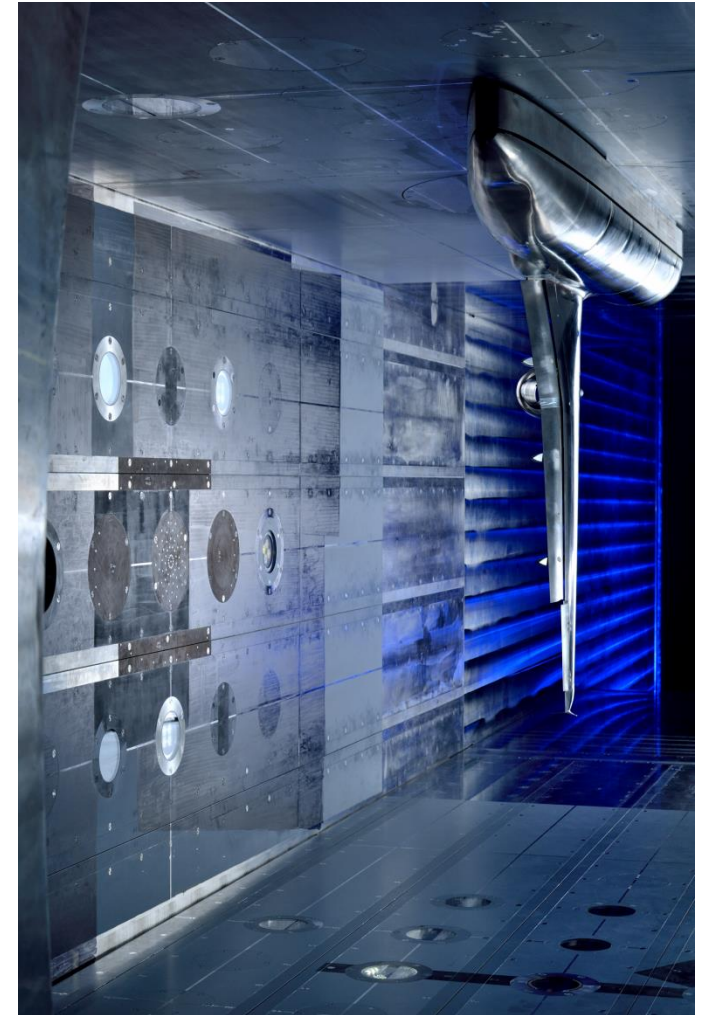
$$110 \text{ kPa} < p_{stat} < 450 \text{ kPa}$$



Setup

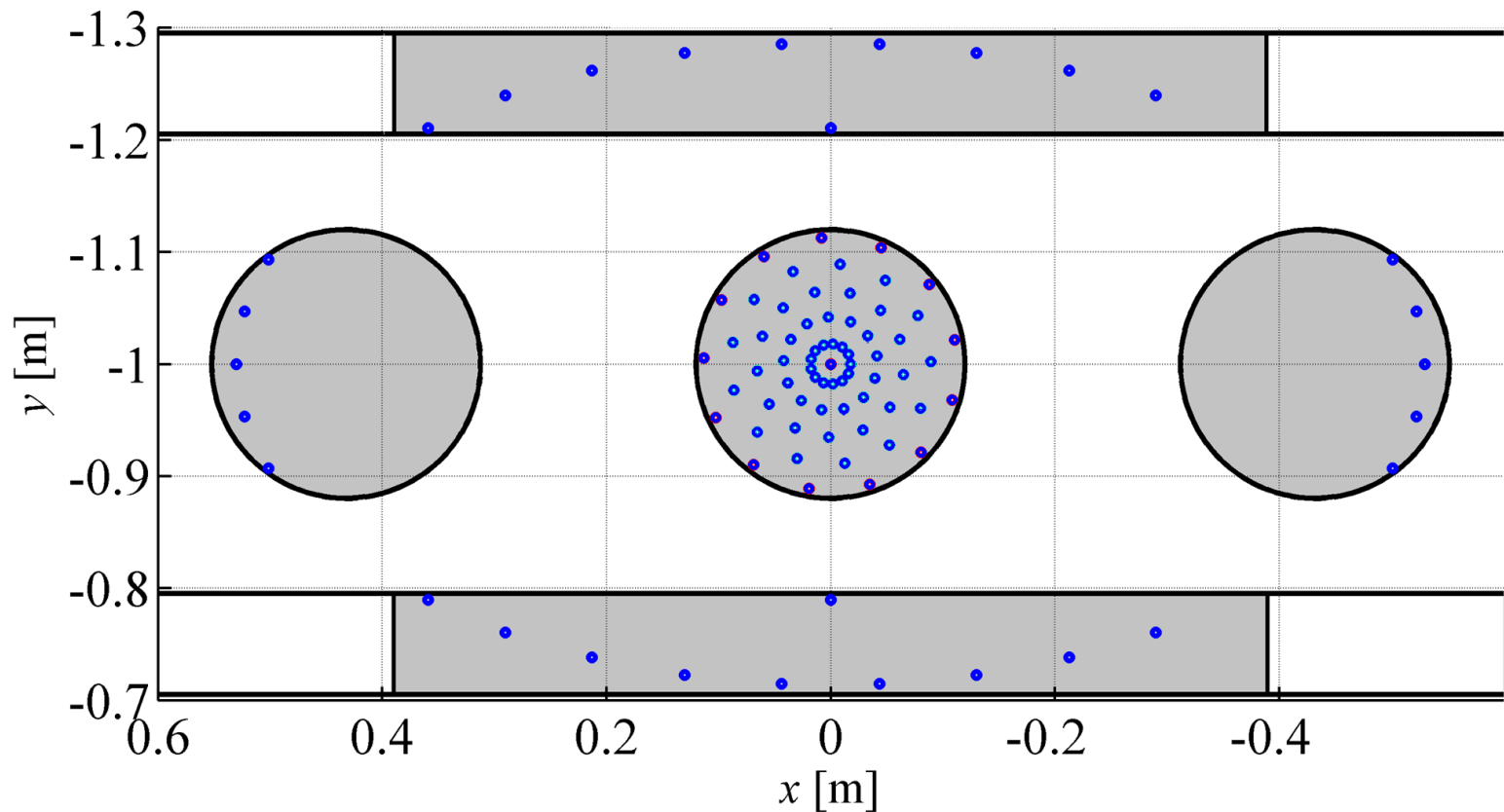
Airbus K3DY half-model

- Scale: 1:13.6 (7.35%), $\delta \approx 0.3$ m
- Slat: 26 deg, Flaps: 34 deg
- High-lift configuration identical to EWA-Benchmark test 2007 at LSWT



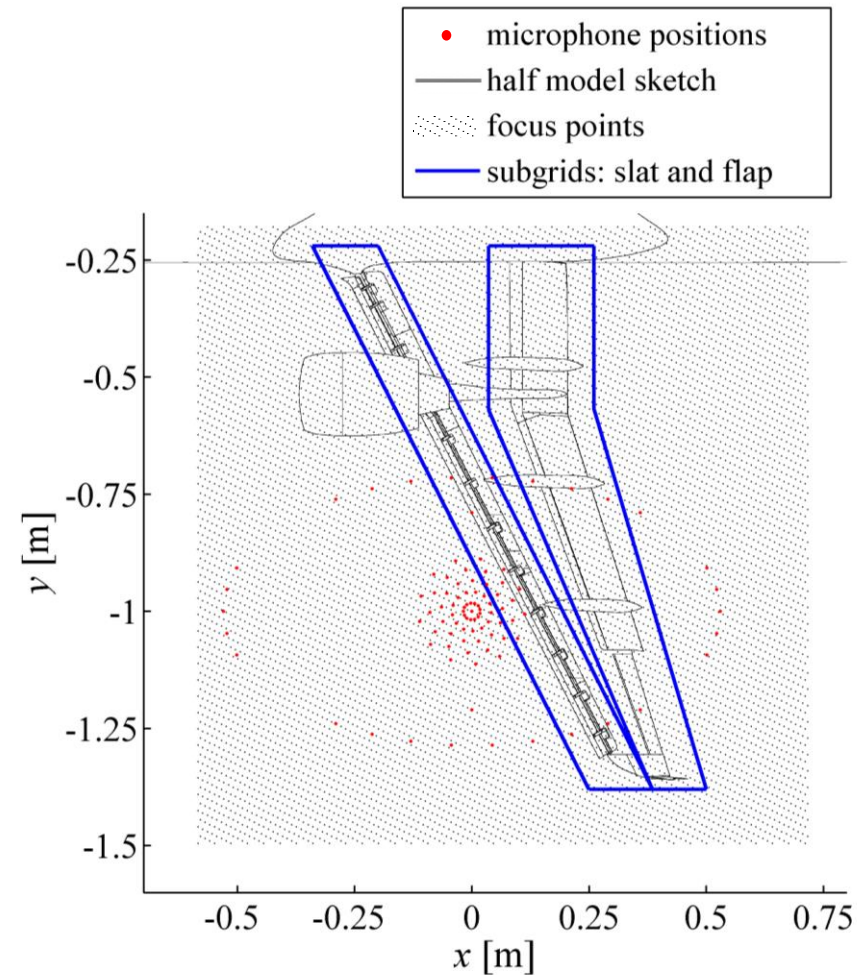
Setup

- Limited positioning of microphones:
 - Significantly restricted angle/area of observation



Data processing

- Algorithms:
 - Conventional beamforming with DR
 - Increased dynamic range: CLEAN-SC*
- Speed of sound: function of temperature and pressure
- Observation plane: 1.30 m × 1.32 m ($d_{xy} = 5$ mm, 69165 grid points)
- Grid rotated with α and dihedral angle



*Sijtsma P., "CLEAN based on spatial source coherence", *International Journal of Aeroacoustics*, Vol 6, 2012.

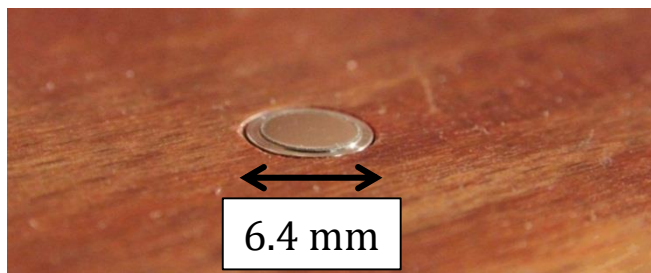
Setup

Microphone-Array

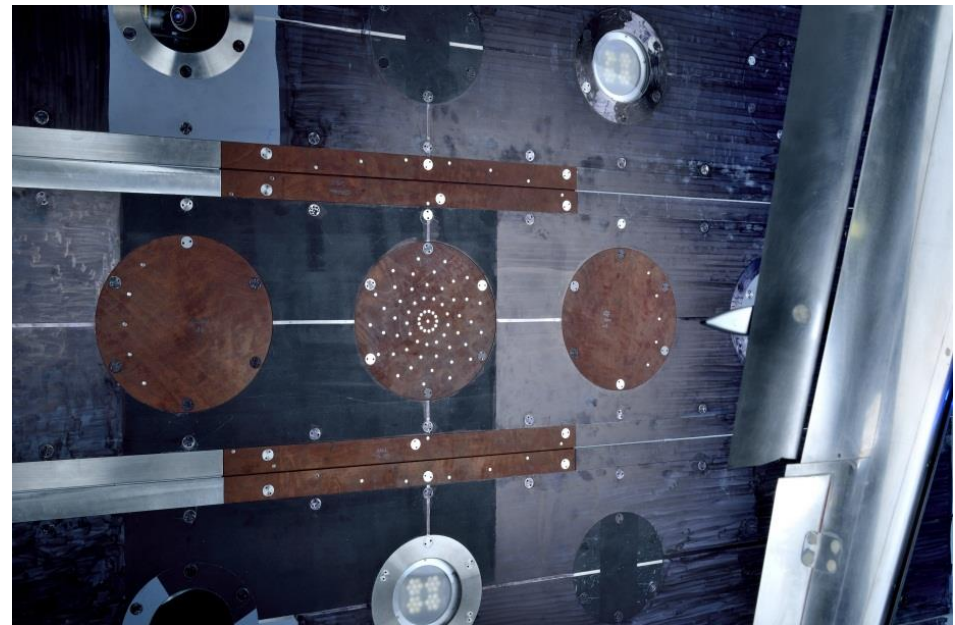
- 96 microphones (flush mounted)
- Inserts: compressed laminated wood



Brüel&Kjær cryogenic-type 4944A

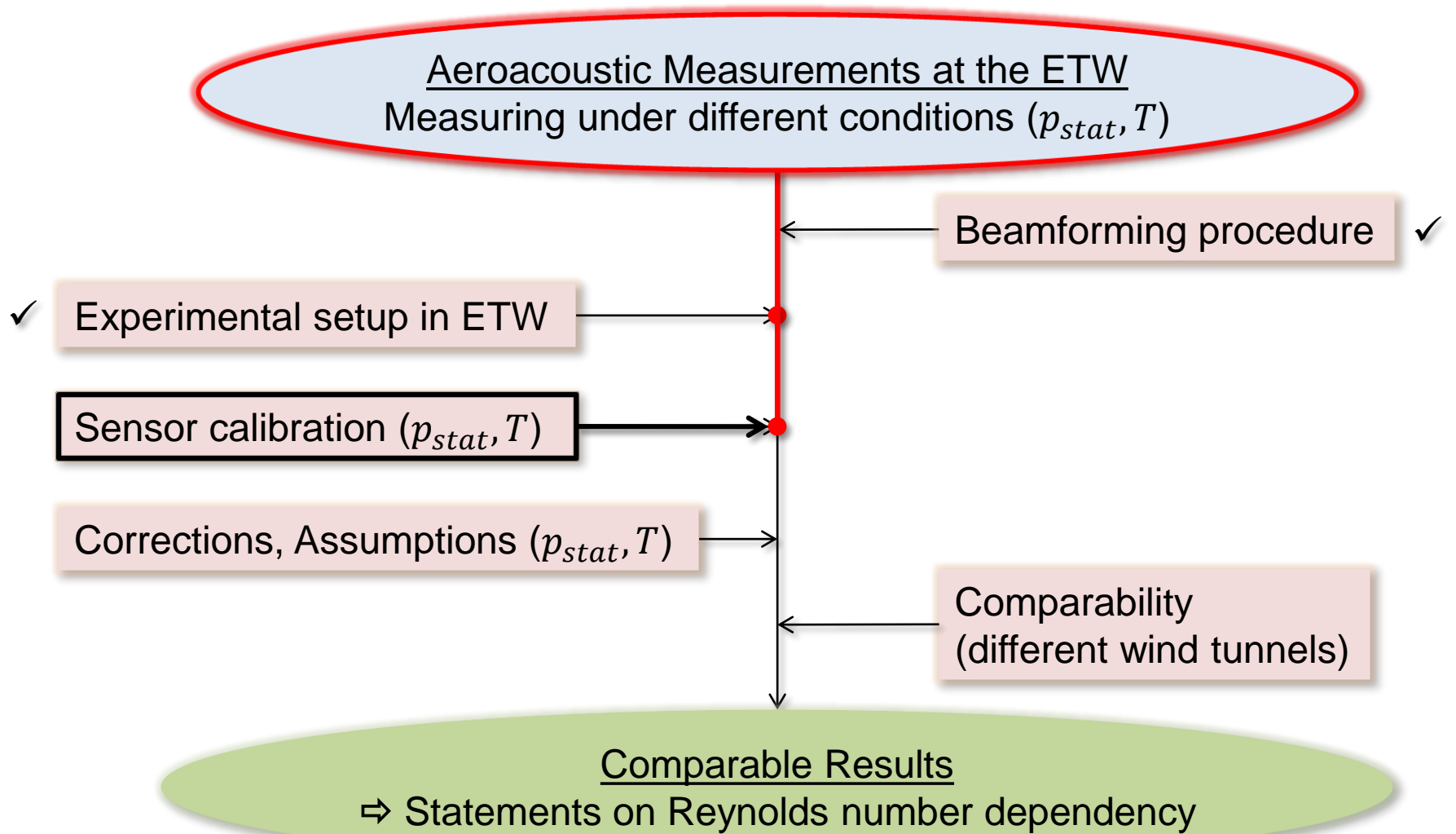


Microphone membrane on test section wall



Microphone array integrated in test section wall





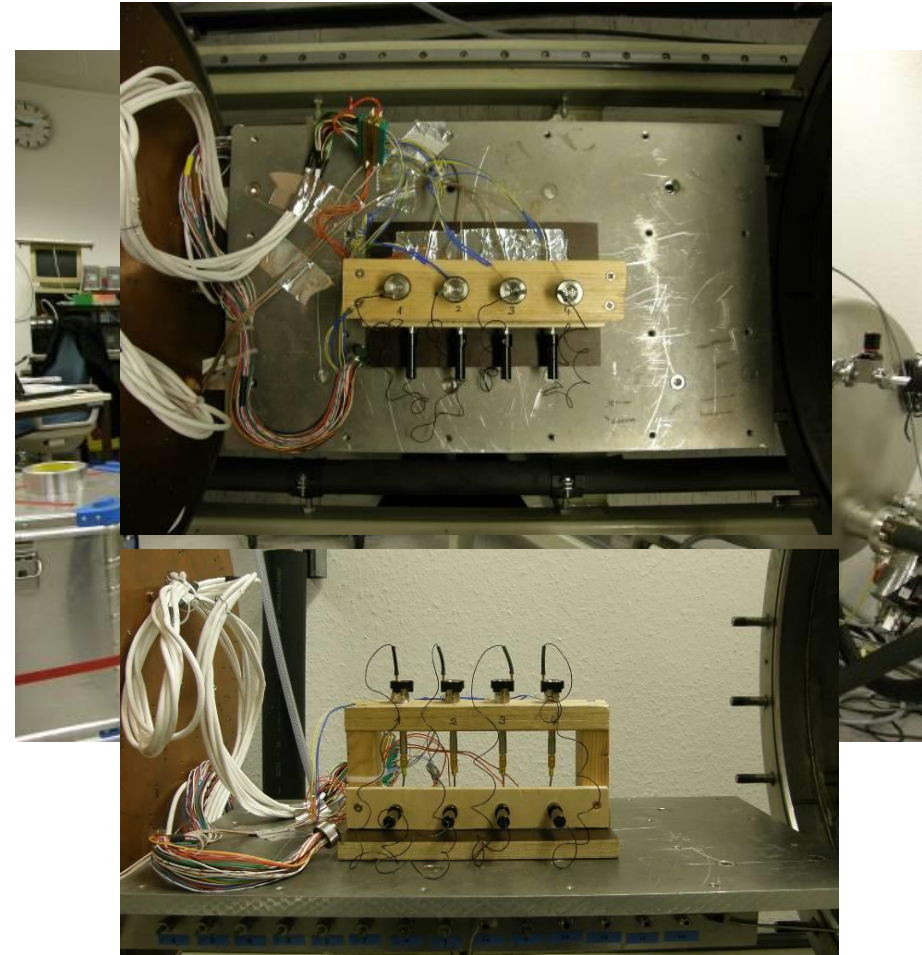
Sensor calibration

Cryogenic vessel of the ETW

- $120 \text{ K} \leq T \leq 290 \text{ K}$
- $100 \text{ kPa} \leq p_{stat} \leq 400 \text{ kPa}$

Measurements

- 4 microphones
(B&K cryogenic-type 4944A)
- PULSE measurement system
(Brüel&Kjær)
- Excitation: electrostatic actuator
 $f_{exc} = 1 \text{ kHz to } 100 \text{ kHz}$



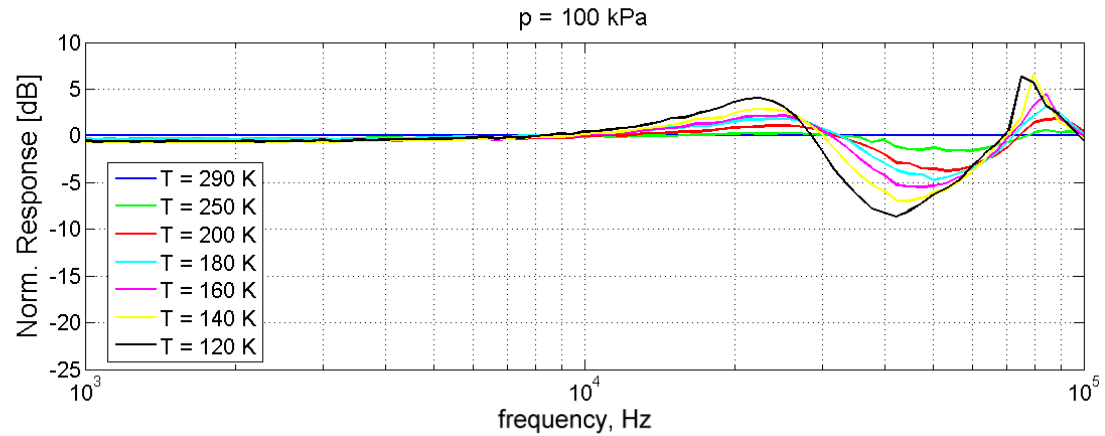
Ahlefeldt T. and Quest J. "High-Reynolds Number Aeroacoustic Testing under Pressurized Cryogenic Conditions in PETW", 50th AIAA-ASM, 2012

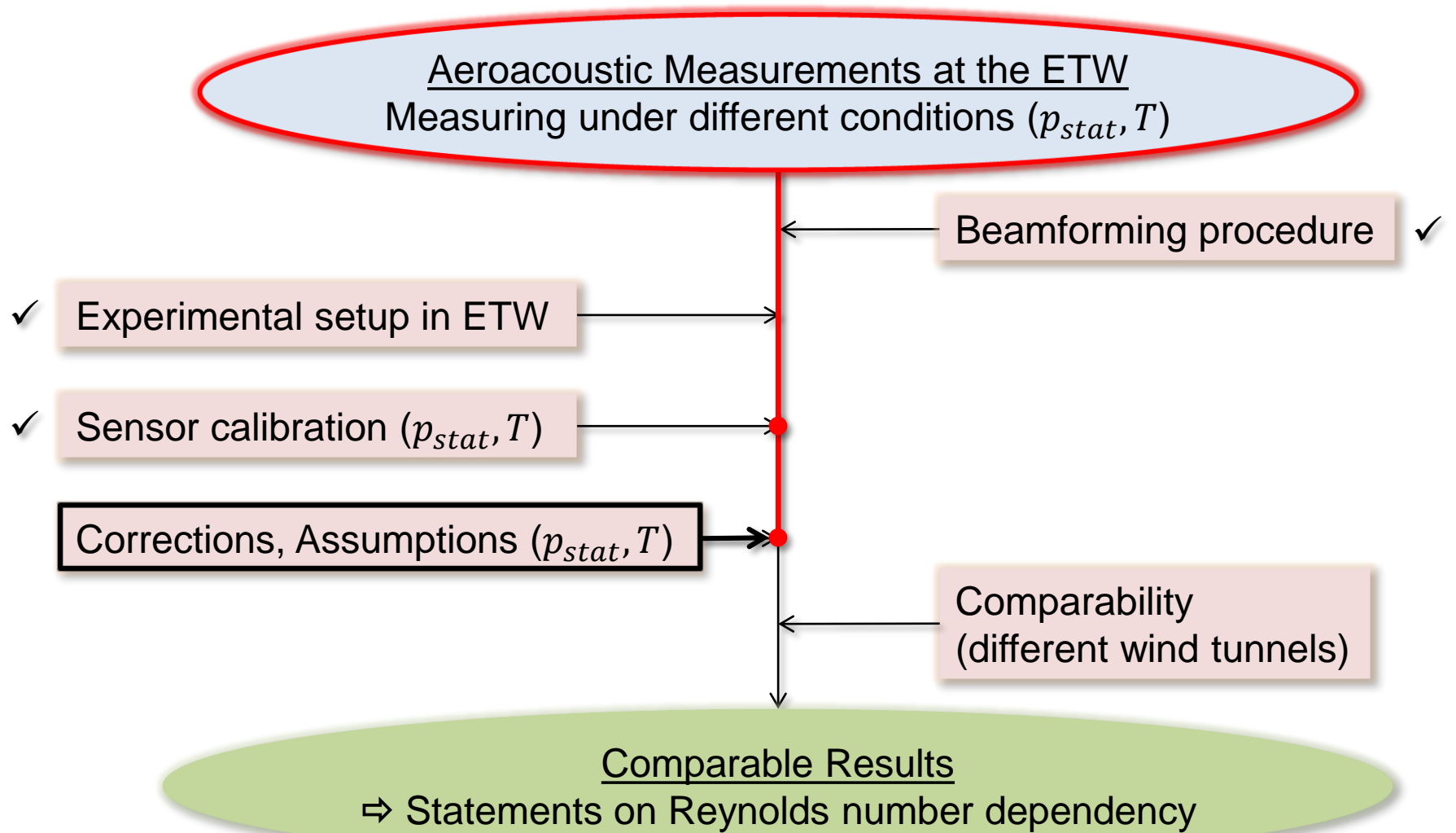


Sensor calibration – frequency response

$p_{stat} = 100 \text{ kPa}$
 $120 \text{ K} \leq T \leq 290 \text{ K}$

- wavy frequency response with several resonances





$$M = u/c$$

$$St = fD/u$$

$$Re = 2\pi fD/c$$

Corrections / Assumptions

- Aeroacoustic similarity:
Reynolds number, Mach number, Strouhal number, (Helmholtz number)
- Conditions
 - Change of static pressure p_{stat} and temperature T
 - $M = \frac{u}{c} = const.$

⇒ Change of density ρ , speed of sound c , flow speed u , Reynolds number Re

Source mechanisms: $p' = \text{function}(\text{frequency}, \text{amplitude}, \text{Reynolds number})$

$c, u \Rightarrow St$

ρ, c, u



Corrections / Assumptions

Amplitude

Dipole*

- Compact source in far-field:

$$I \propto \frac{\rho u_{\infty}^6}{c^3} \frac{D^2}{r^2} f(Re)$$

*Curle N., "The Influence of Solid Boundaries upon Aerodynamic Sound", *Proc. R. Soc. Lond., A*, Vol 231 (1955).

#Lighthill M.J., "On sound generated aerodynamically I. General theory", *Proc. R. Soc. Lond., A*, Vol 211 (1952).

Ahlefeldt T., "Aeroacoustic Measurements of a Scaled Half-Model at High Reynolds Numbers", *AIAA Journal*, Vol. 55, No. 1 (2017).



Corrections / Assumptions

- Aeroacoustic similarity:
Reynolds number, Mach number, Strouhal number, (Helmholtz number)
- Source mechanisms: $p' = \text{function}(\text{frequency}, \text{amplitude}, \text{Reynolds number})$
- Comparison at $M = \text{const.}$

Diagram illustrating the relationship between the Strouhal number (St) and the acoustic pressure level (ΔdB).

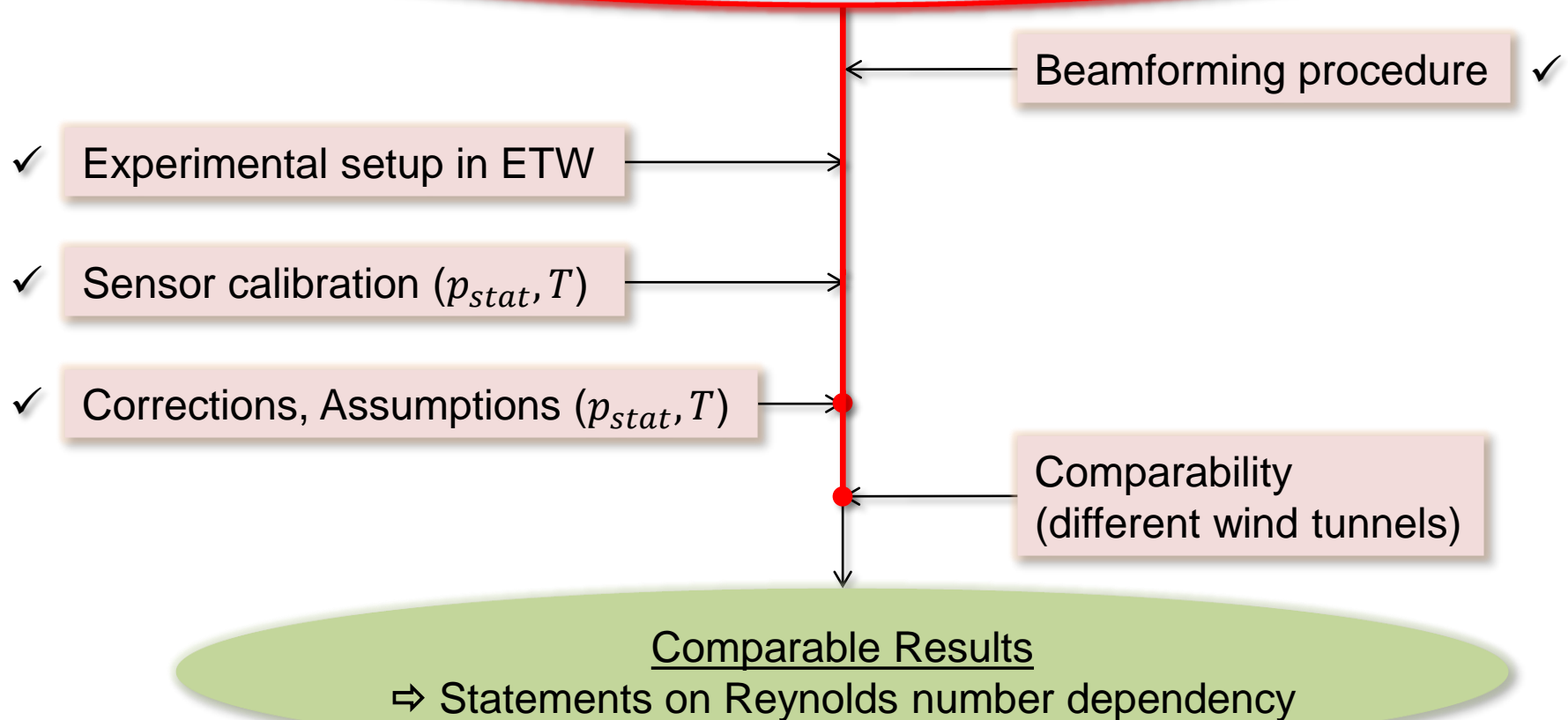
The Strouhal number (St) is shown in a circle, connected by a line to the term "frequency" in the function definition above. The parameters ρ, c, u are shown in an oval, connected by a line to the term "amplitude" in the function definition above.

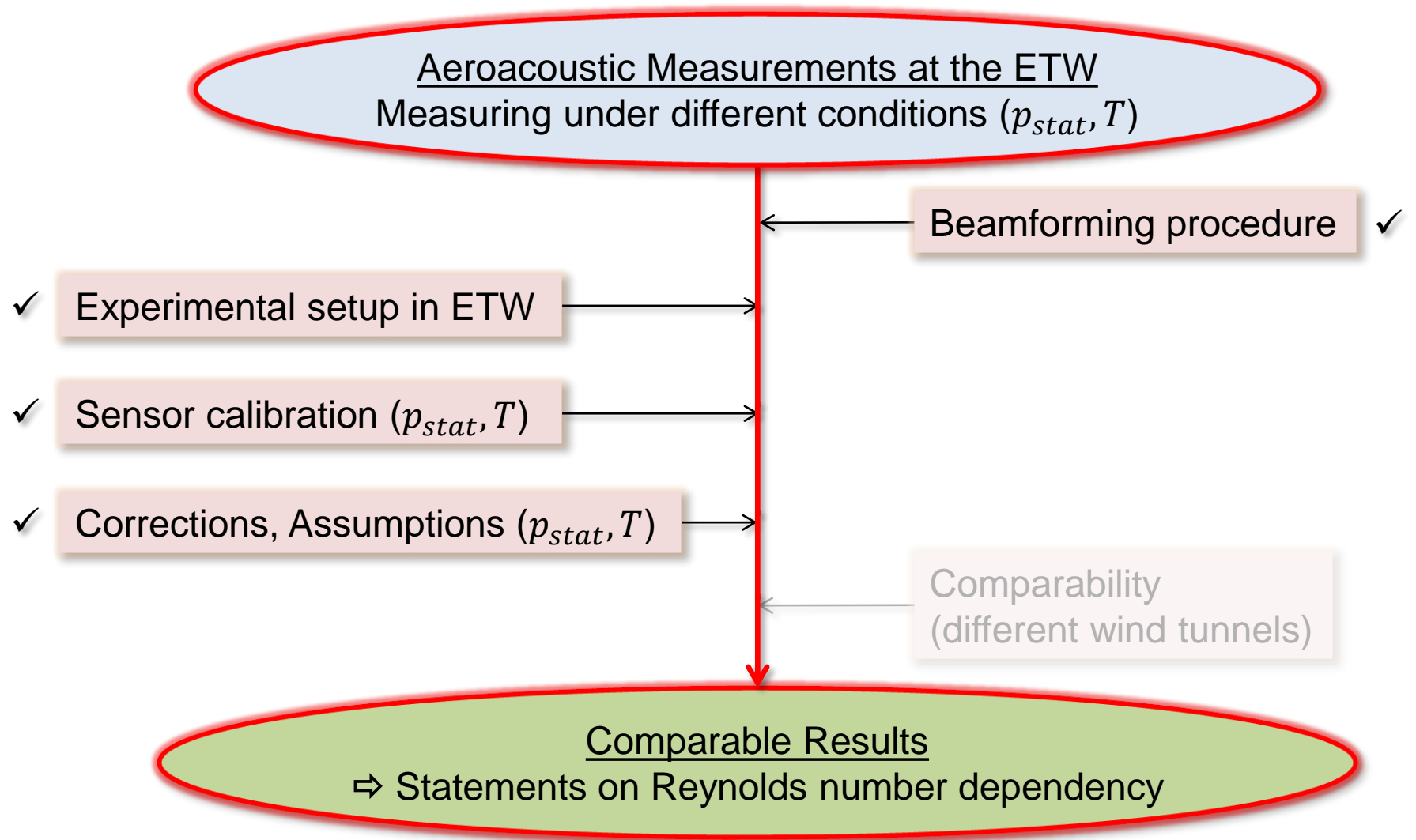
The acoustic pressure level is given by the equation:

$$\Delta dB = 20 \log_{10} \left(\frac{\rho c^2}{\rho_0 c_0^2} \right)$$



Aeroacoustic Measurements at the ETW
Measuring under different conditions (p_{stat}, T)





Results – Source maps (CLEAN-SC)

$M = 0.203$ | $\alpha = 3^\circ$ | *Variation of Strouhal number*

$$Re_\delta = 1.42 \cdot 10^6$$

$$Re_\delta = 5.16 \cdot 10^6$$

$$Re_\delta = 20.0 \cdot 10^6$$



Results – Source maps (CLEAN-SC)

$M = 0.203 \mid \alpha = 3^\circ \mid$ Variation of Strouhal number

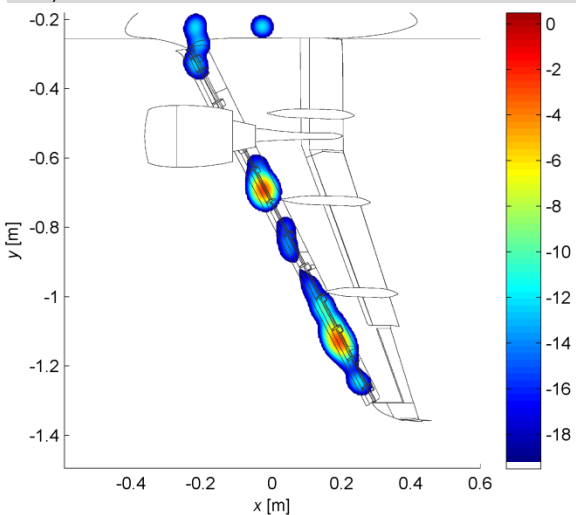
$$St_{\delta,1/30ct} = 20 \mid f_{full-scale} = 335 \text{ Hz}$$

$$Re_\delta = 1.42 \cdot 10^6$$

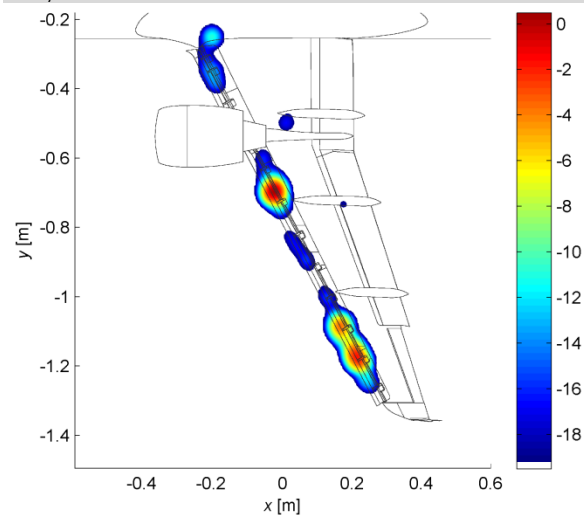
$$Re_\delta = 5.16 \cdot 10^6$$

$$Re_\delta = 20.0 \cdot 10^6$$

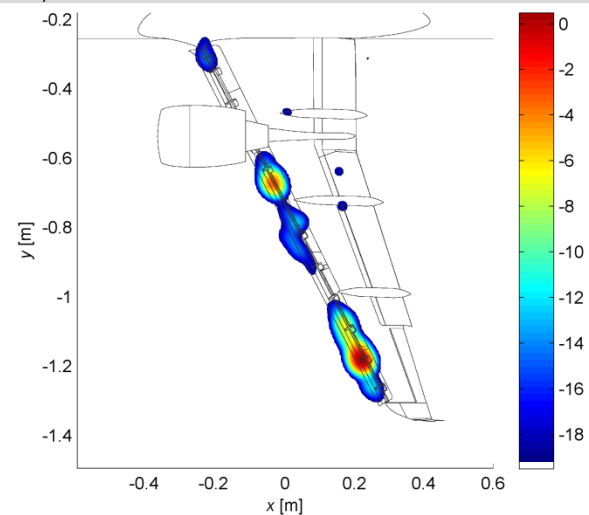
$St_{1/30ct} = 20$ (4.7 kHz) | $T = 311 \text{ K}$ | $p = 110 \text{ kPa}$



$St_{1/30ct} = 20$ (4.8 kHz) | $T = 311 \text{ K}$ | $p = 399 \text{ kPa}$



$St_{1/30ct} = 20$ (3.0 kHz) | $T = 120 \text{ K}$ | $p = 419 \text{ kPa}$



Quantitative comparison (identical scale), corrections applied



Results – Source maps (CLEAN-SC)

$M = 0.203 \mid \alpha = 3^\circ \mid$ Variation of Strouhal number

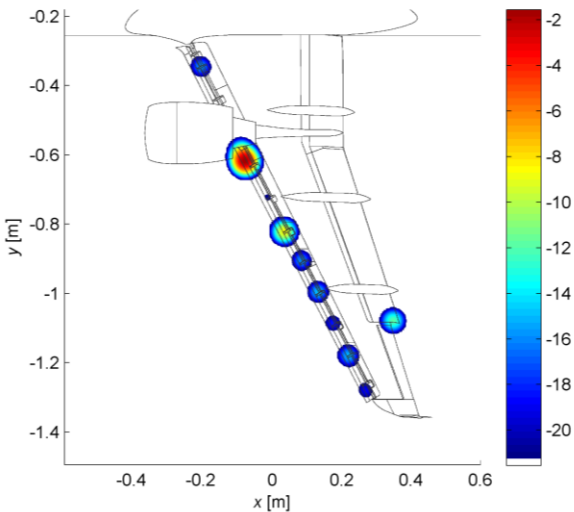
$$St_{\delta,1/30ct} = 70 \mid f_{full-scale} = 1.2 \text{ kHz}$$

$$Re_\delta = 1.42 \cdot 10^6$$

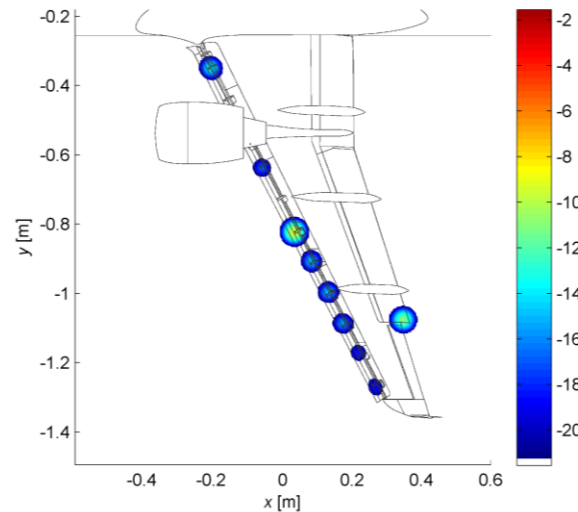
$$Re_\delta = 5.16 \cdot 10^6$$

$$Re_\delta = 20.0 \cdot 10^6$$

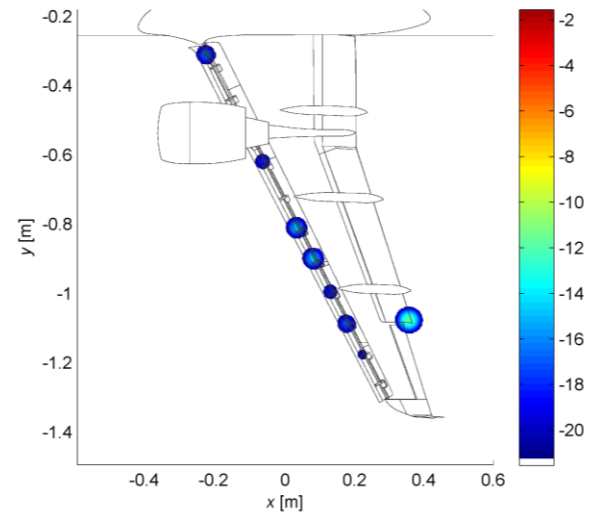
$St_{1/30ct} = 70$ (16.5 kHz) | $T = 311 \text{ K}$ | $p = 110 \text{ kPa}$



$St_{1/30ct} = 70$ (16.6 kHz) | $T = 311 \text{ K}$ | $p = 399 \text{ kPa}$



$St_{1/30ct} = 70$ (10.5 kHz) | $T = 120 \text{ K}$ | $p = 419 \text{ kPa}$



Quantitative comparison (identical scale), corrections applied



Results – Source maps (CLEAN-SC)

$M = 0.203 \mid \alpha = 3^\circ \mid$ Variation of Strouhal number

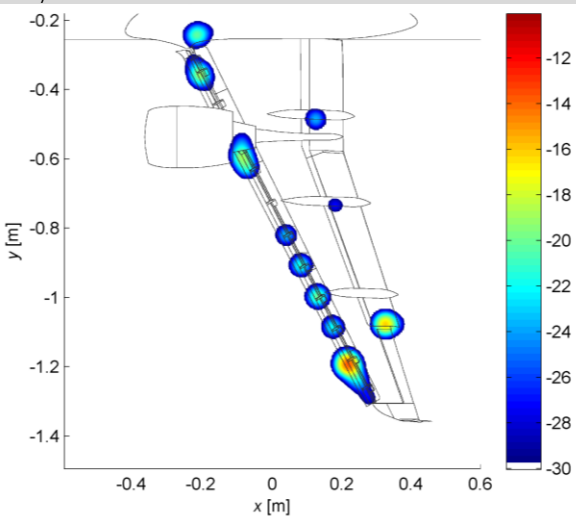
$$St_{\delta,1/30ct} = 130 \mid f_{full-scale} = 2.2 \text{ kHz}$$

$$Re_\delta = 1.42 \cdot 10^6$$

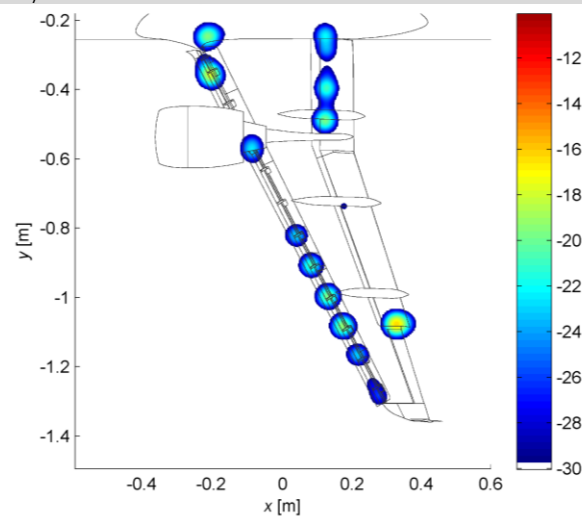
$$Re_\delta = 5.16 \cdot 10^6$$

$$Re_\delta = 20.0 \cdot 10^6$$

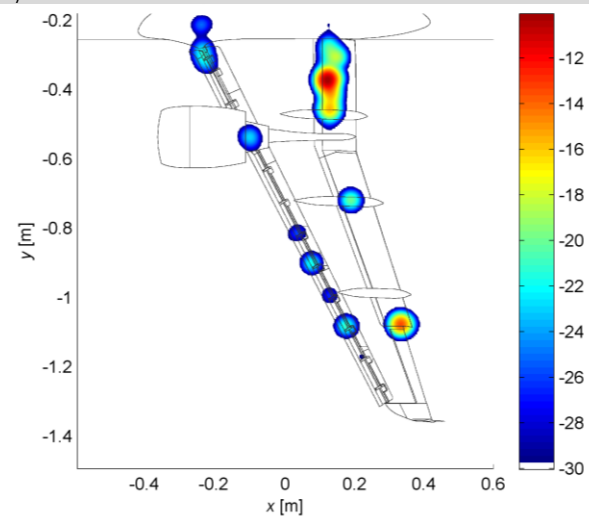
$St_{1/30ct} = 130$ (30.7 kHz) | $T = 311 \text{ K}$ | $p = 110 \text{ kPa}$



$St_{1/30ct} = 130$ (30.9 kHz) | $T = 311 \text{ K}$ | $p = 399 \text{ kPa}$



$St_{1/30ct} = 130$ (19.6 kHz) | $T = 120 \text{ K}$ | $p = 419 \text{ kPa}$



Quantitative comparison (identical scale), corrections applied



Results – Source maps (CLEAN-SC)

$M = 0.203 \mid \alpha = 3^\circ \mid$ Variation of Strouhal number

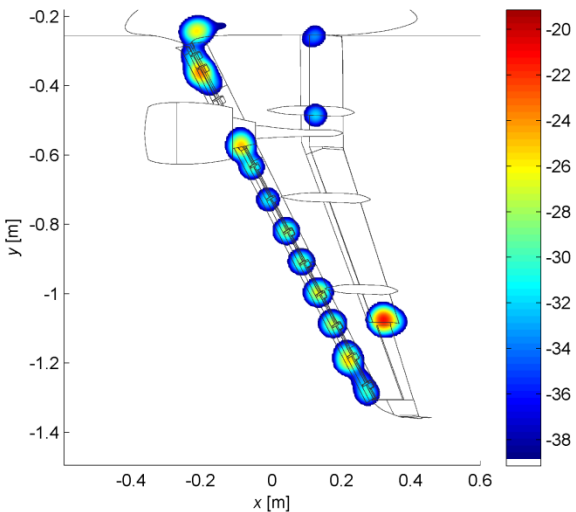
$$St_{\delta,1/30ct} = 200 \mid f_{full-scale} = 3.4 \text{ kHz}$$

$$Re_\delta = 1.42 \cdot 10^6$$

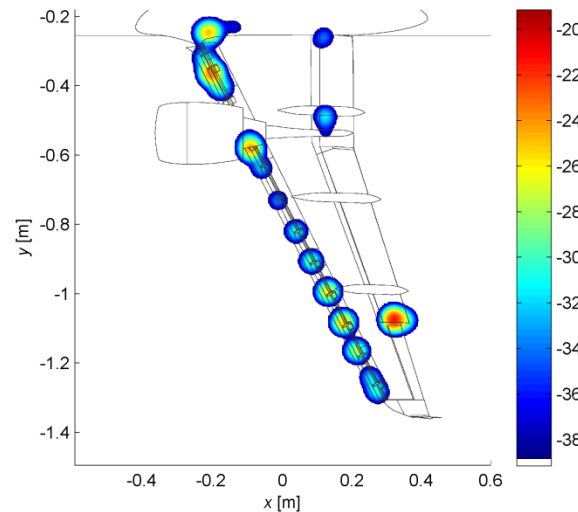
$$Re_\delta = 5.16 \cdot 10^6$$

$$Re_\delta = 20.0 \cdot 10^6$$

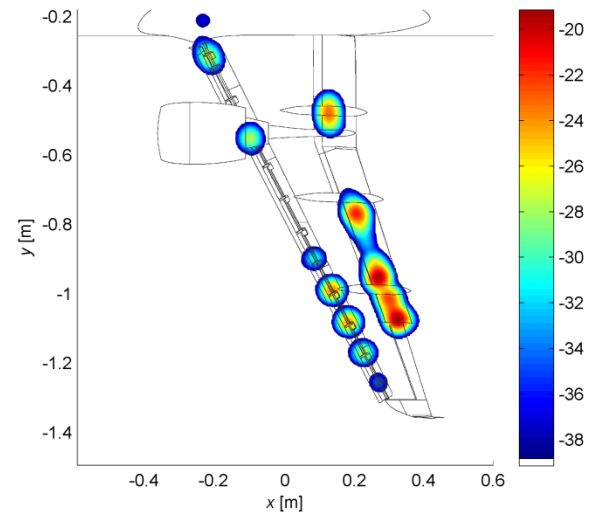
$St_{1/30ct} = 200$ (47.3 kHz) | $T = 311 \text{ K}$ | $p = 110 \text{ kPa}$



$St_{1/30ct} = 200$ (47.5 kHz) | $T = 311 \text{ K}$ | $p = 399 \text{ kPa}$



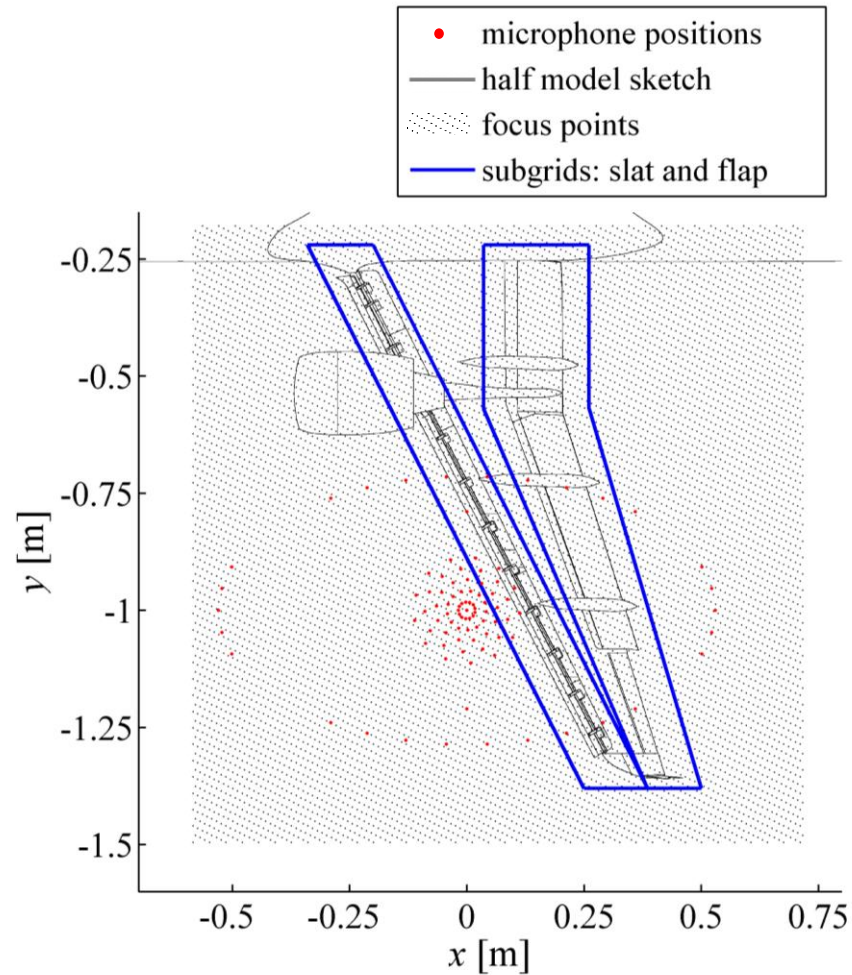
$St_{1/30ct} = 200$ (30.1 kHz) | $T = 120 \text{ K}$ | $p = 419 \text{ kPa}$



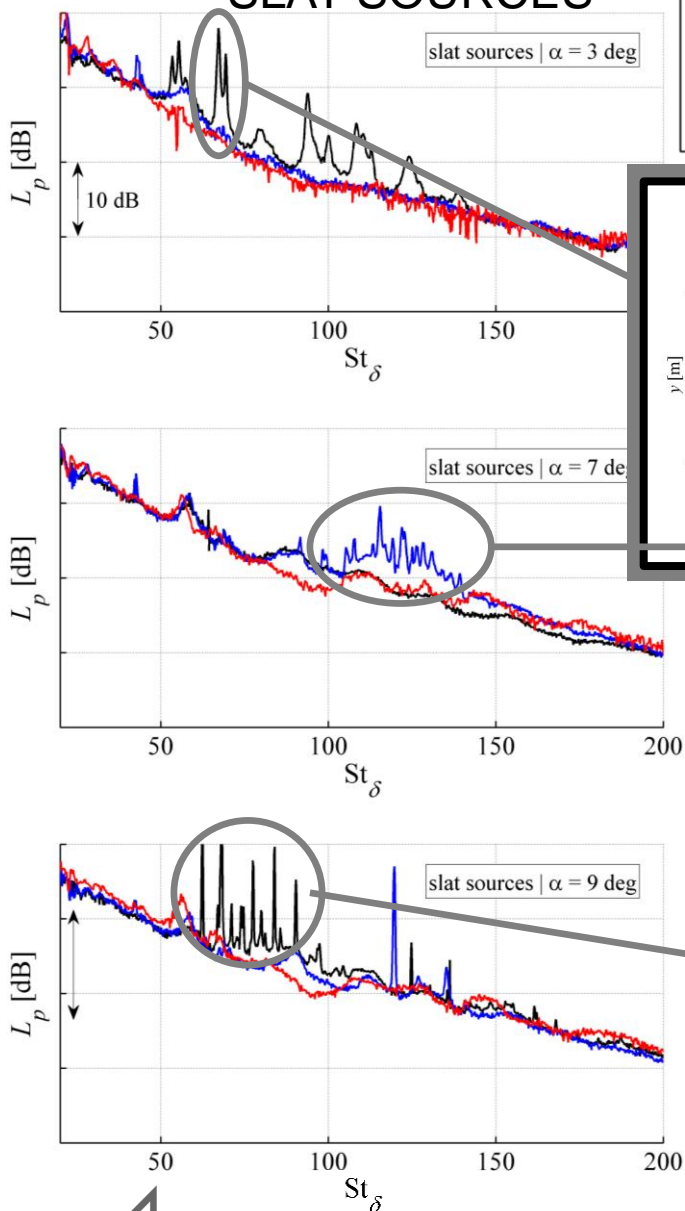
Quantitative comparison (identical scale), corrections applied



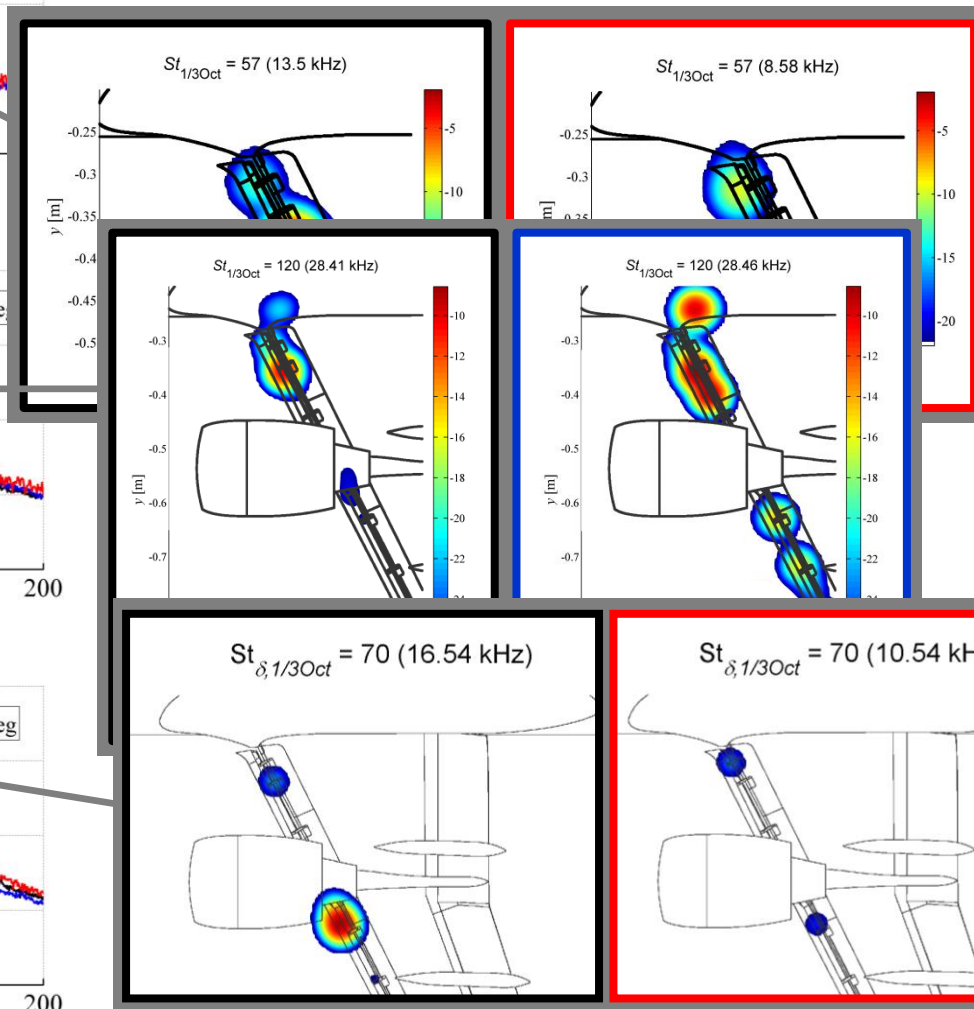
Results – Spectra: flap and slat

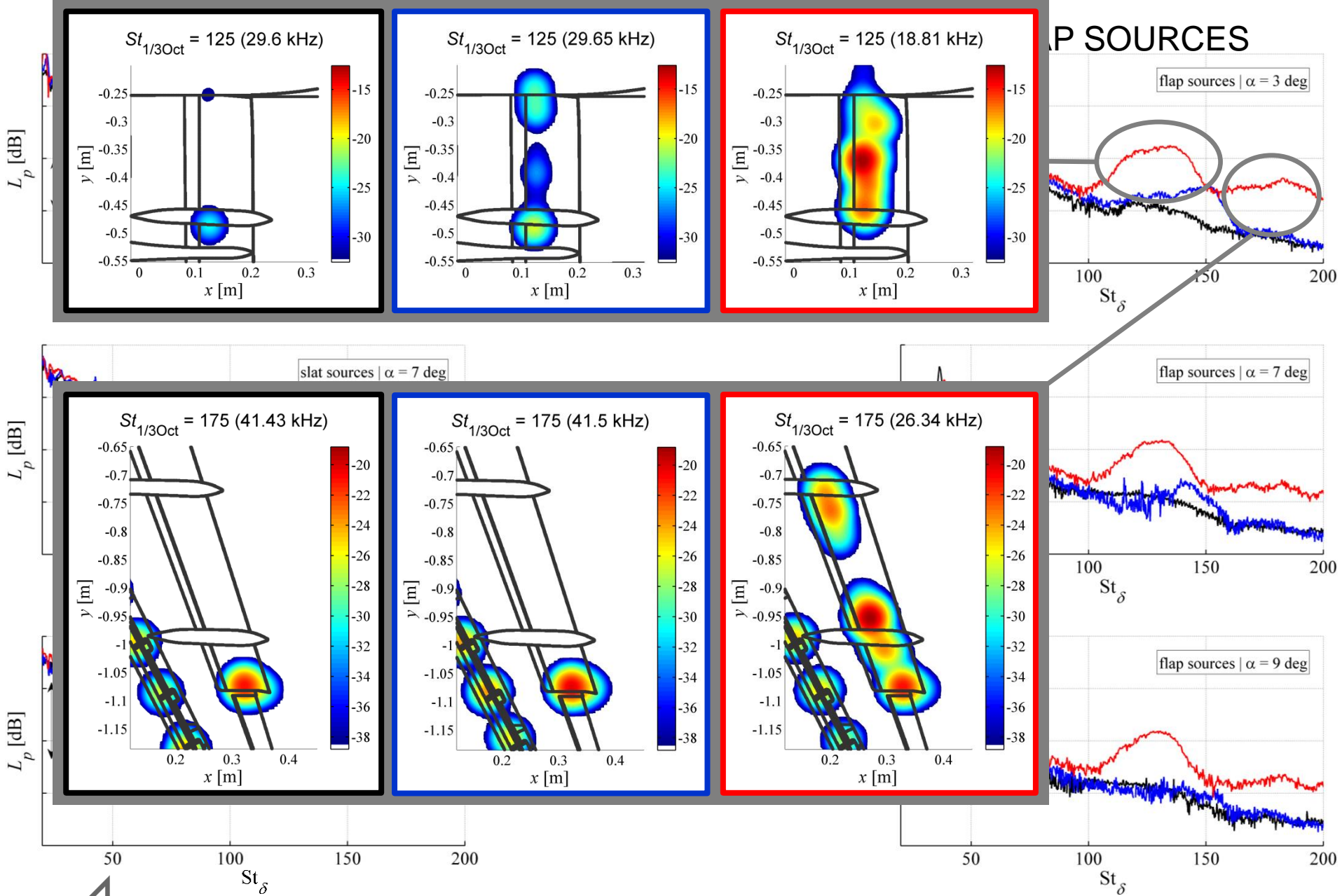


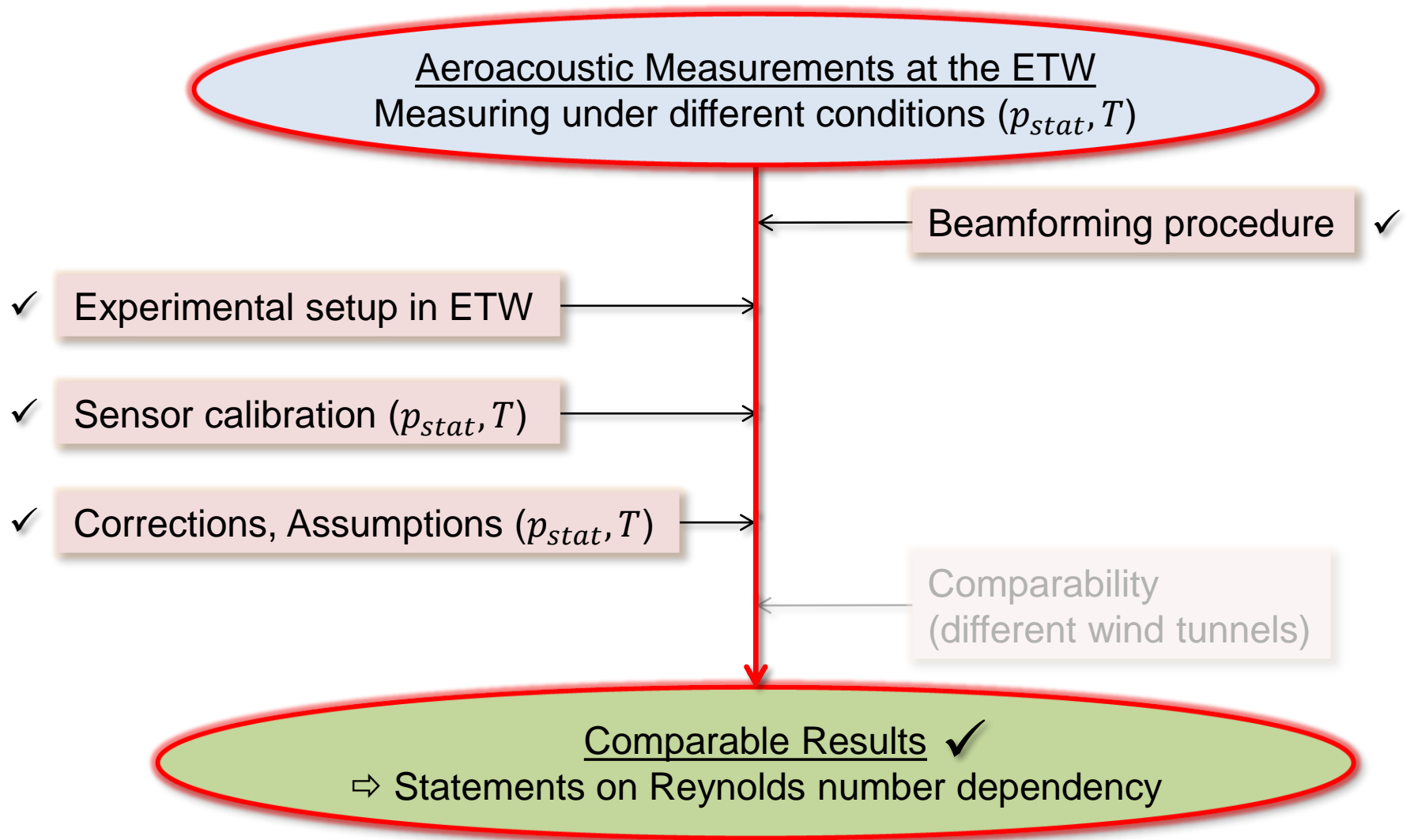
SLAT SOURCES



— DP I: $Re_\delta = 1.43 \cdot 10^6$ | $q/E = 1.55 \cdot 10^{-8}$
 — DP III: $Re_\delta = 5.17 \cdot 10^6$ | $q/E = 5.64 \cdot 10^{-8}$
 — DP IV: $Re_\delta = 20.06 \cdot 10^6$ | $q/E = 5.64 \cdot 10^{-8}$





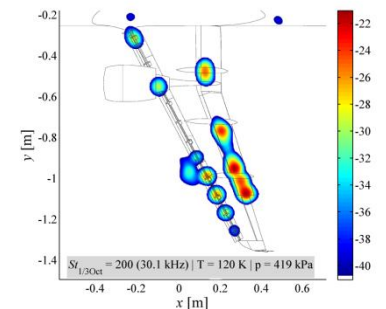
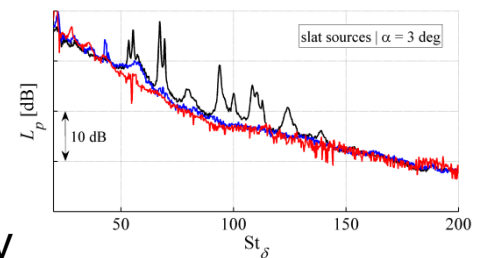


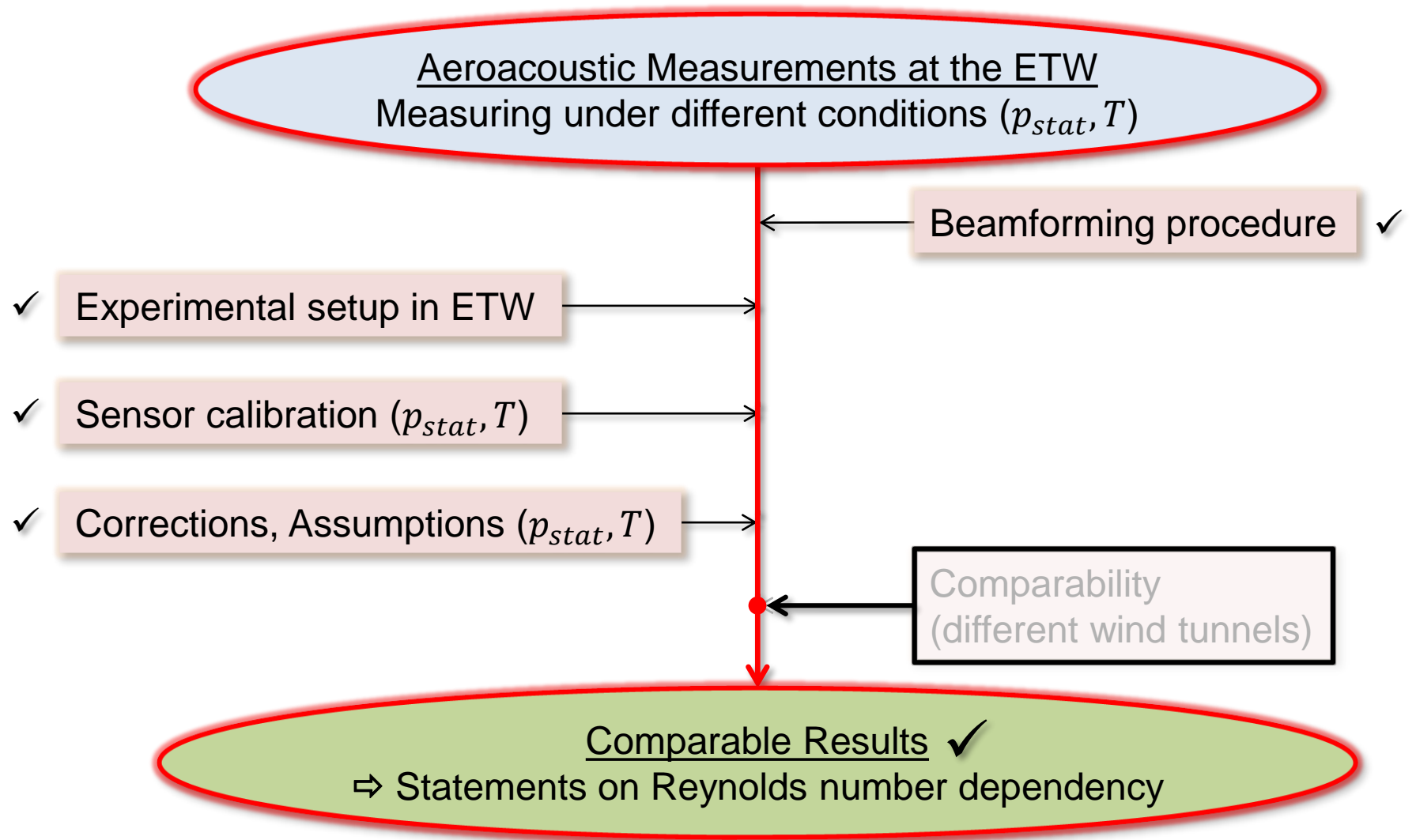
Summary

- Small-scale model airframe noise data at real-flight Reynolds numbers

- Significant Reynolds number dependencies

- $St_\delta < 100$ ($f_{full-scale} < 1,8 \text{ kHz}$):
 - Slat tones at low Re
 - Various peaks with combined Re & St dependency
- $St_\delta > 100$ ($f_{full-scale} < 1,8 \text{ kHz}$):
 - Inboard slat sources at mid-level Re
 - Dominant broadband peaks on flap at real-flight Re

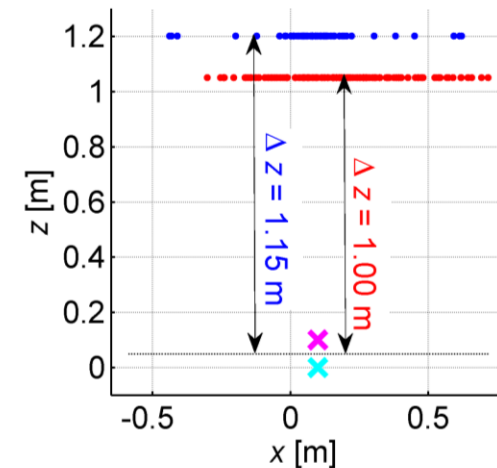
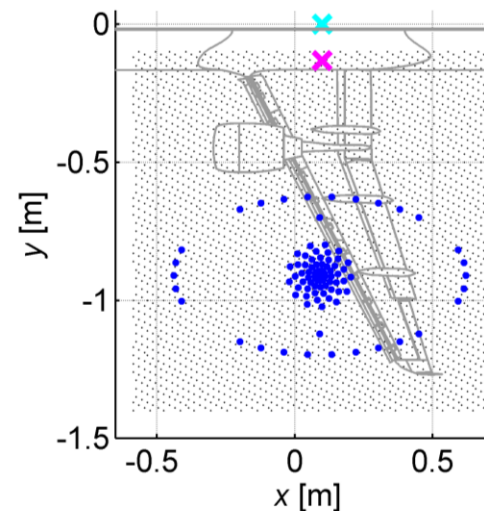
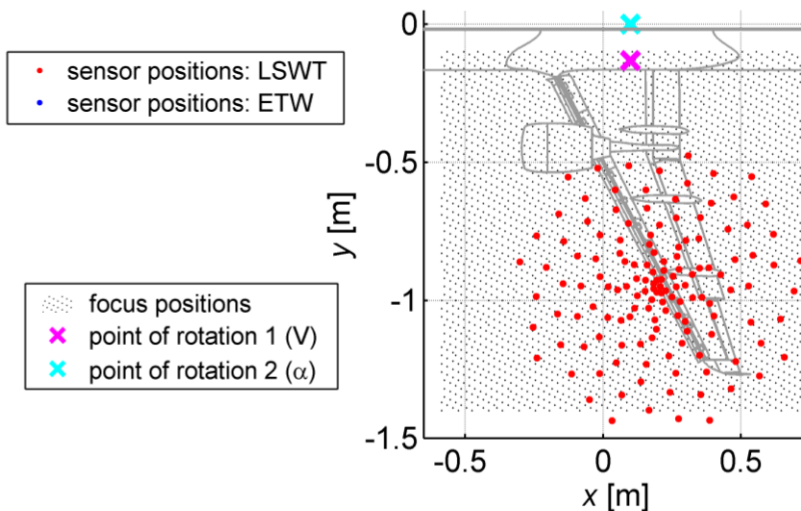
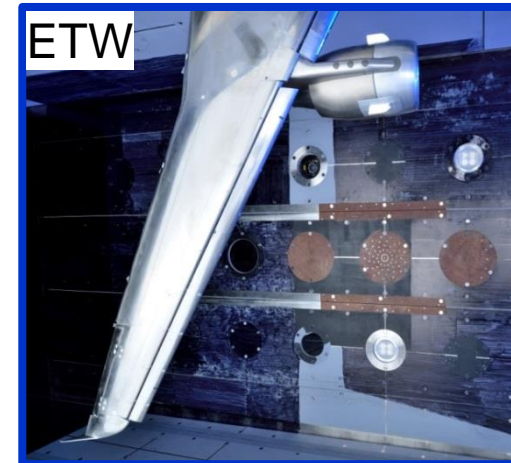




Comparability – Setup



- Identical model
- Identical configuration
- Identical flow parameter (Low Reynolds number)
- Different wind tunnels
- Different microphone arrays
- Different microphones

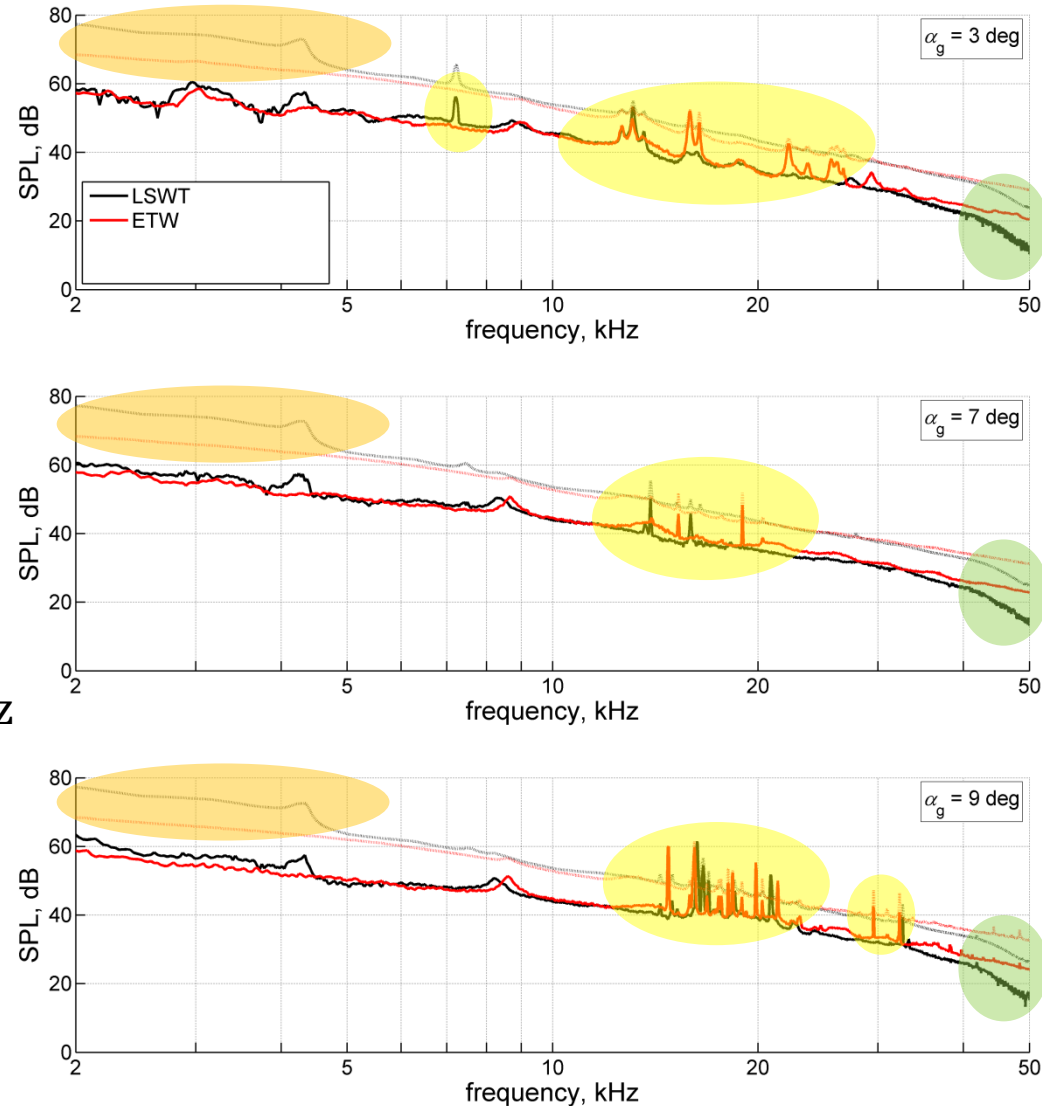


Spehr C. and Ahlefeldt T., "Comparison of Microphone Array Measurements in the Closed Test Section of LSWT and ETW", *CEAS Journal*, accepted for publication (2018).



Comparability – spectra

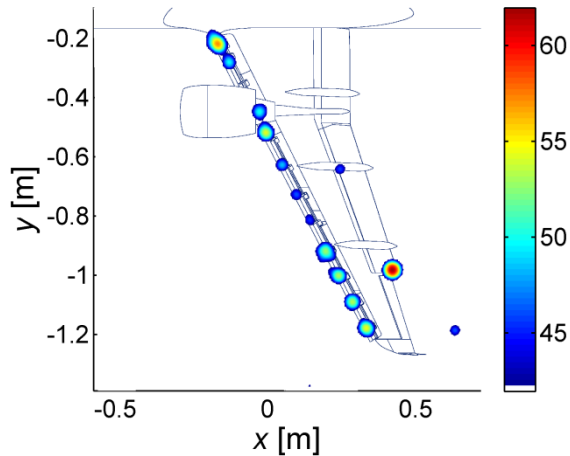
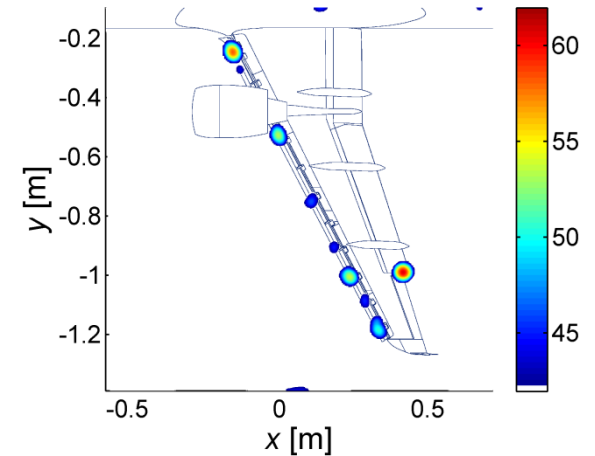
- Overall spectra similar: $\pm 2\text{dB}$
- Increased Background noise at LSWT \Rightarrow peak at $\approx 3.2\text{ kHz}$
- Differences for tonal components (“slat tones”)
- Differences at frequencies $> 40\text{ kHz}$ \Rightarrow microphone calibration



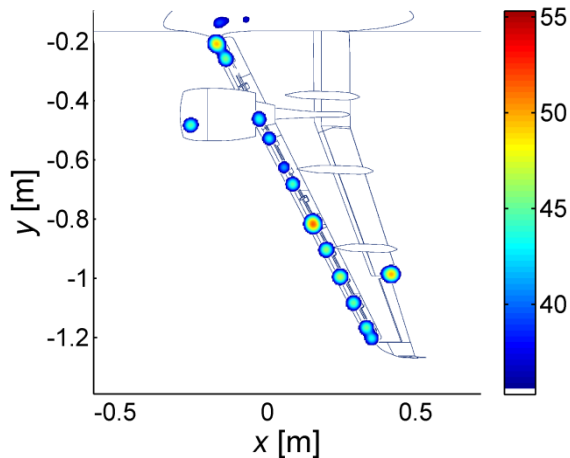
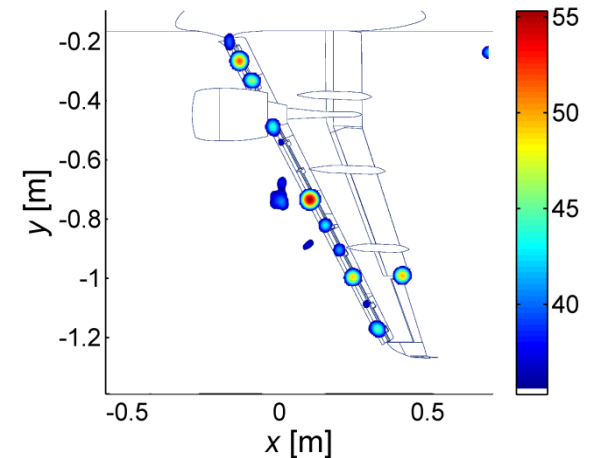
Spehr C. and Ahlefeldt T., “Comparison of Microphone Array Measurements in the Closed Test Section of LSWT and ETW”, *CEAS Journal*, accepted for publication (2018).



Comparability – source maps

LSWT $f_{1/3\text{Oct}} = 8 \text{ kHz}$ **ETW** $f_{1/3\text{Oct}} = 8 \text{ kHz}$ 

- Main sources are at same positions with minor differences in level

 $f_{1/3\text{Oct}} = 16 \text{ kHz}$  $f_{1/3\text{Oct}} = 16 \text{ kHz}$ 

- Sources on slat vary significantly



$Re \approx 1,4 \text{ Mio}$ $Re \approx 5,2 \text{ Mio}$ $Re \approx 20 \text{ Mio}$

Aeroacoustic Measurements at the ETW

Measuring under different conditions (p_{stat}, T)

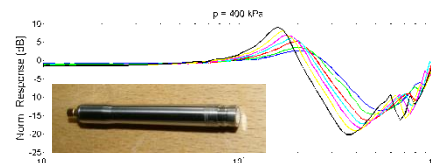
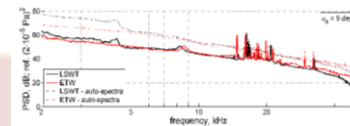
Experimental setup in ETW

Sensor calibration (p_{stat}, T)Corrections, Assumptions (p_{stat}, T)

$$\Delta dB = 20 \log_{10} \left(\frac{\rho c^2}{\rho_0 c_0^2} \right)$$

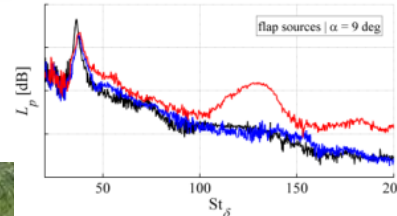
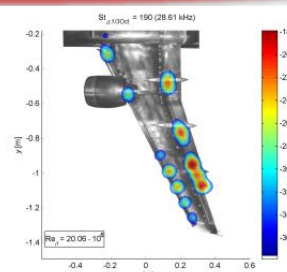
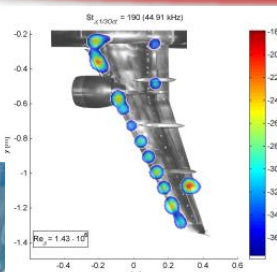
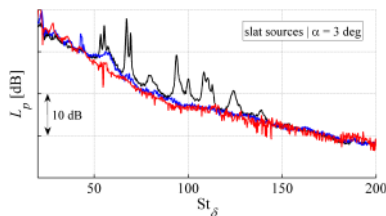
Beamforming procedure

$$B(y, \omega) = \frac{g(y, \omega) * C(\omega) g(y, \omega)}{\|g(y, \omega) g(y, \omega) * \|_F^2}$$

Comparability
(different wind tunnels)

Comparable Results

⇒ Statements on Reynolds number dependency



Take aways

- How do microphone array measurements in WT work
- Corrections and assumptions
- Offer: Sharing data, results and knowledge for cooperation

Questions?
Comments?



Background: acoustic sources in beamforming

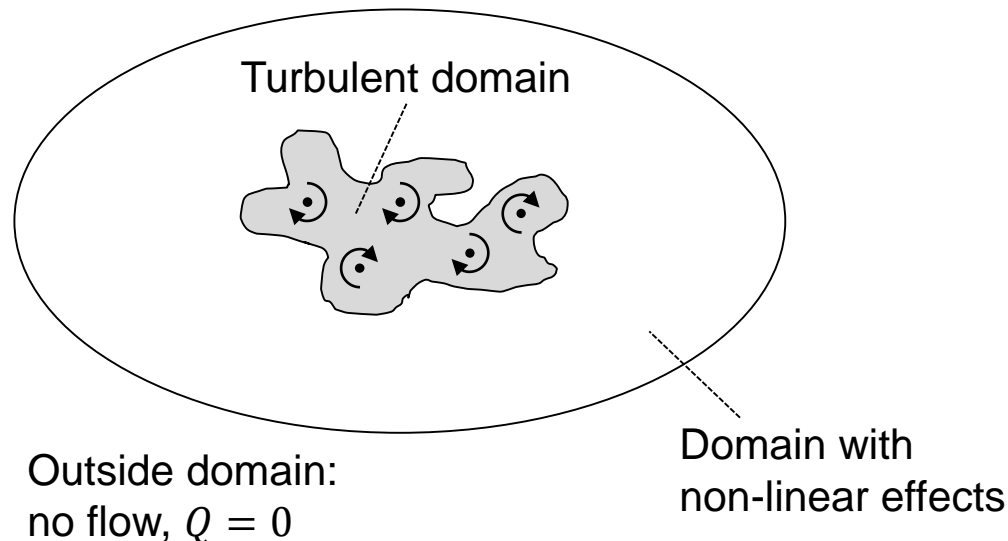
Numerical approach

$$\frac{1}{c^2} \frac{\partial}{\partial t^2} p' - \Delta p' = \sum_{i,j=1}^3 \frac{\partial^2}{\partial x_i \partial x_j} (\rho v_i v_j - \tau_{ij}) + \frac{\partial^2}{\partial t^2} \left(\frac{1}{c^2} p' - \rho' \right)$$

Lighthill equation with fluctuating pressure $p' = p - p_0$

„Equivalent sources“

(contains also kinematic effects: refraction, convection...)



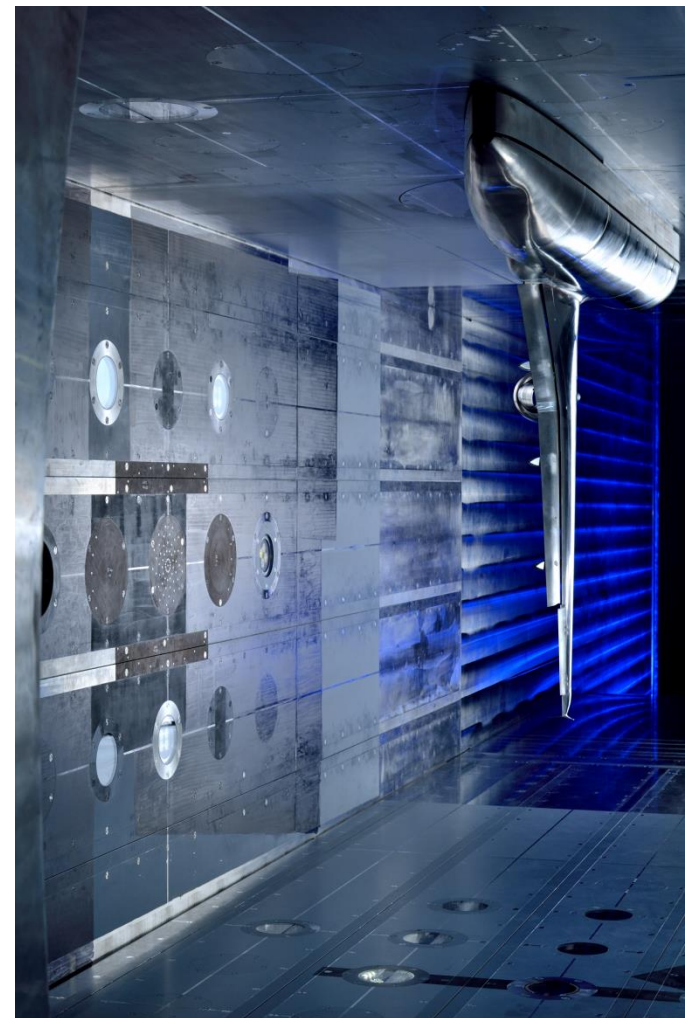
Setup

Airbus K3DY half-model

- Scale: 1:13.6 (7.35%)
- High-lift configuration identical to EWA-Benchmark test 2007 at LSWT

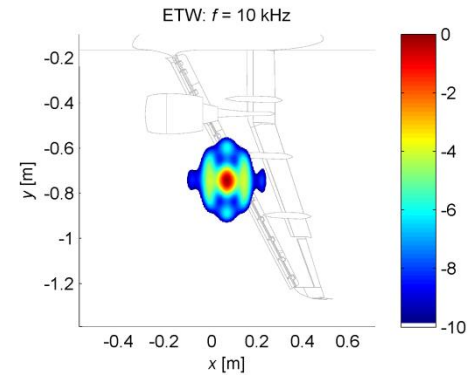
Data points ($M = 0.203$)

	T [K]	p_{stat} [kPa]	Re_δ [10^6]	q/E [10^{-8}]
DP I	310	110	1.42	1.57
DP II	125	115	5.16	1.57
DP III	310	399	5.16	5.70
DP IV	120	419	20.00	5.70

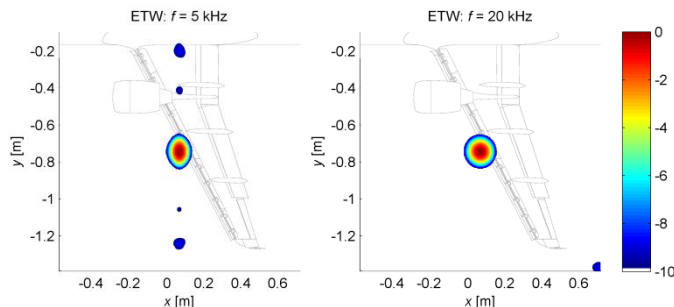


Setup

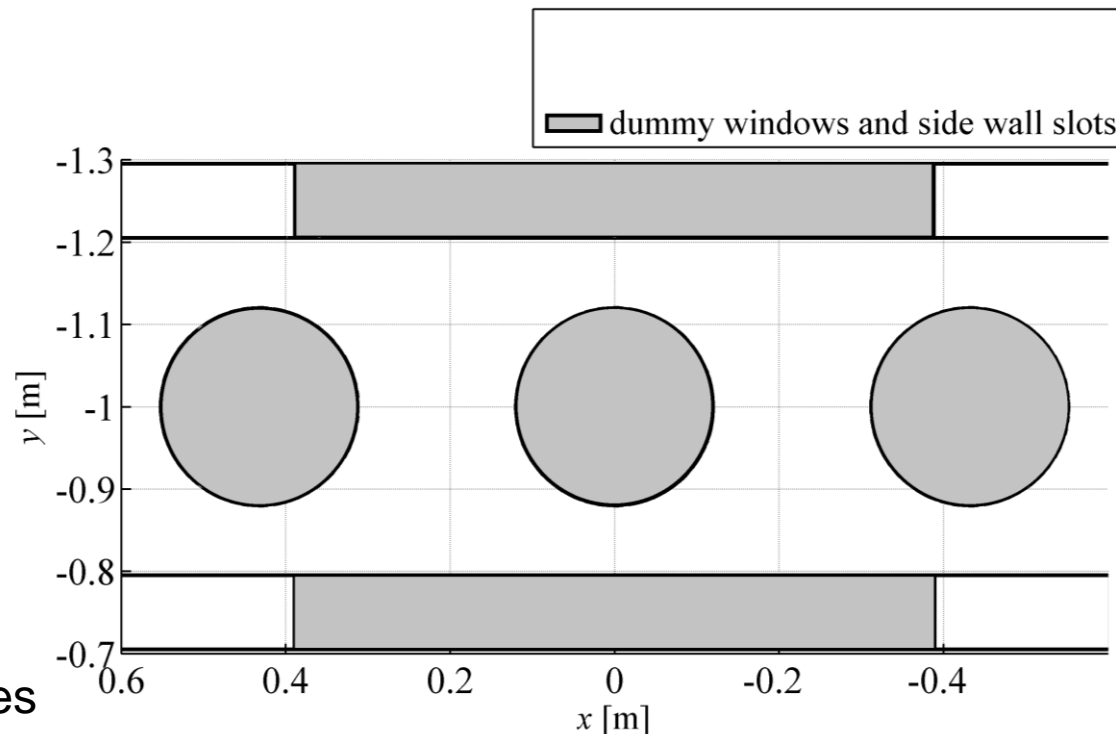
- Limited positioning of microphones:
 - Significantly restricted angle/area of observation
 - Conventional beamforming: strong sidelobes



- Different microphone groups used for conventional maps (“nested arrays”)



- After validation:
 - *CLEAN-SC with all microphones

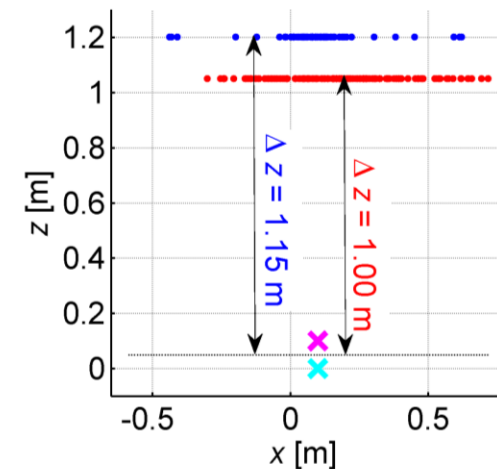
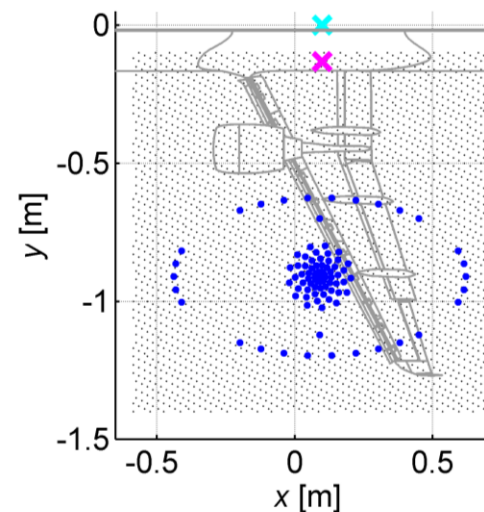
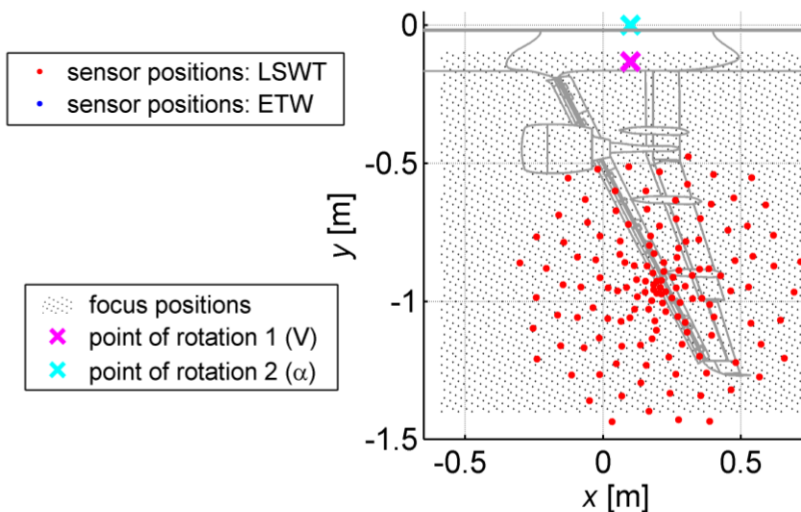
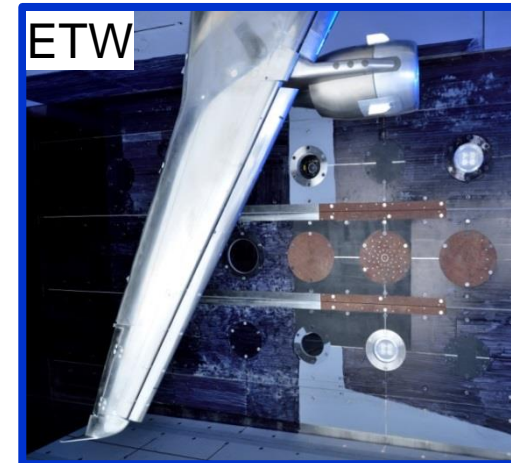


*Sijtsma P., “CLEAN based on spatial source coherence”, *International Journal of Aeroacoustics*, Vol 6, 2012.

Comparability – Setup

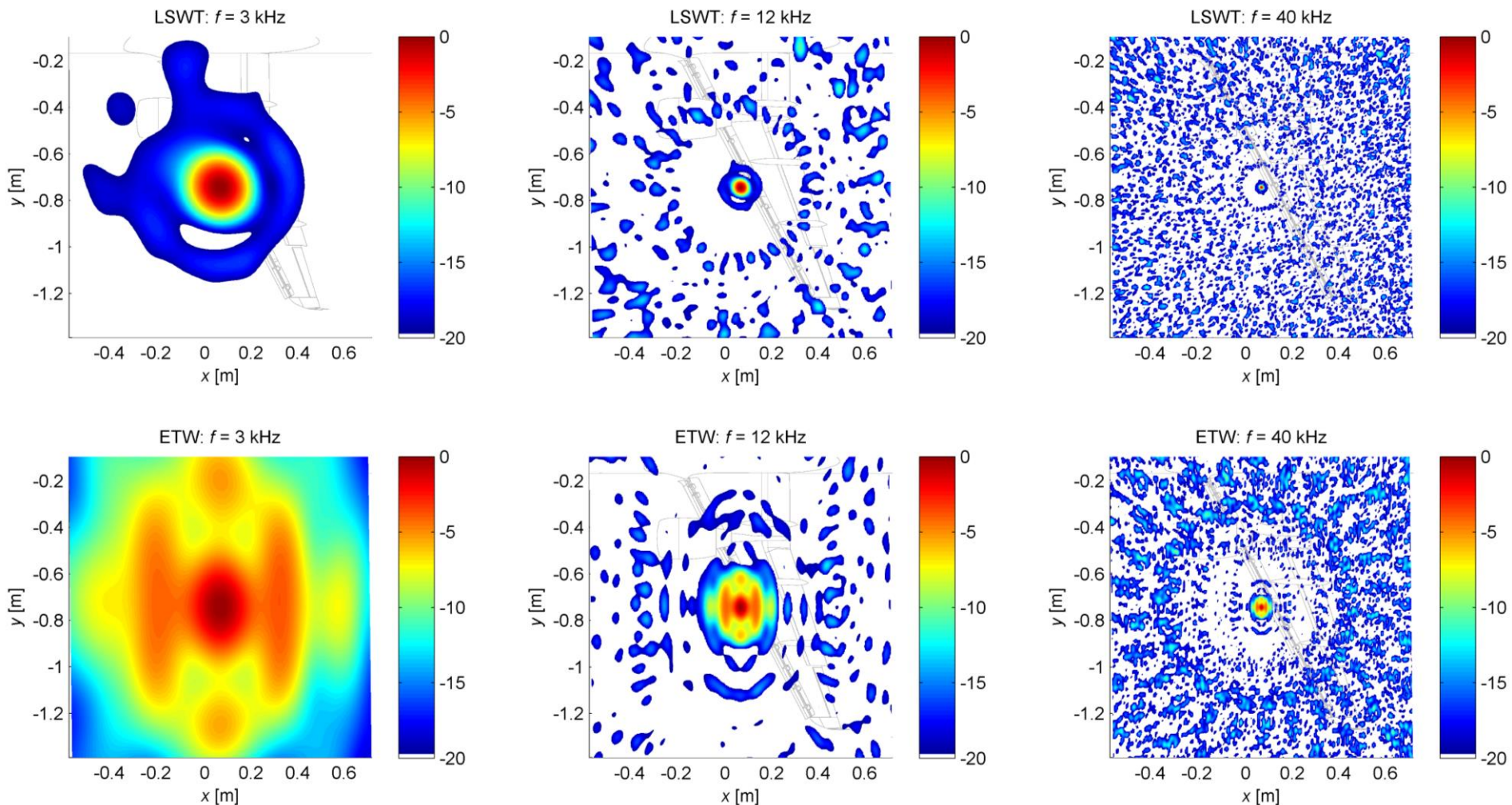


- Identical model
- Identical configuration
- Identical flow parameter (Low Reynolds number)
- Different wind tunnels (but similar dimensions)
- Different microphone arrays



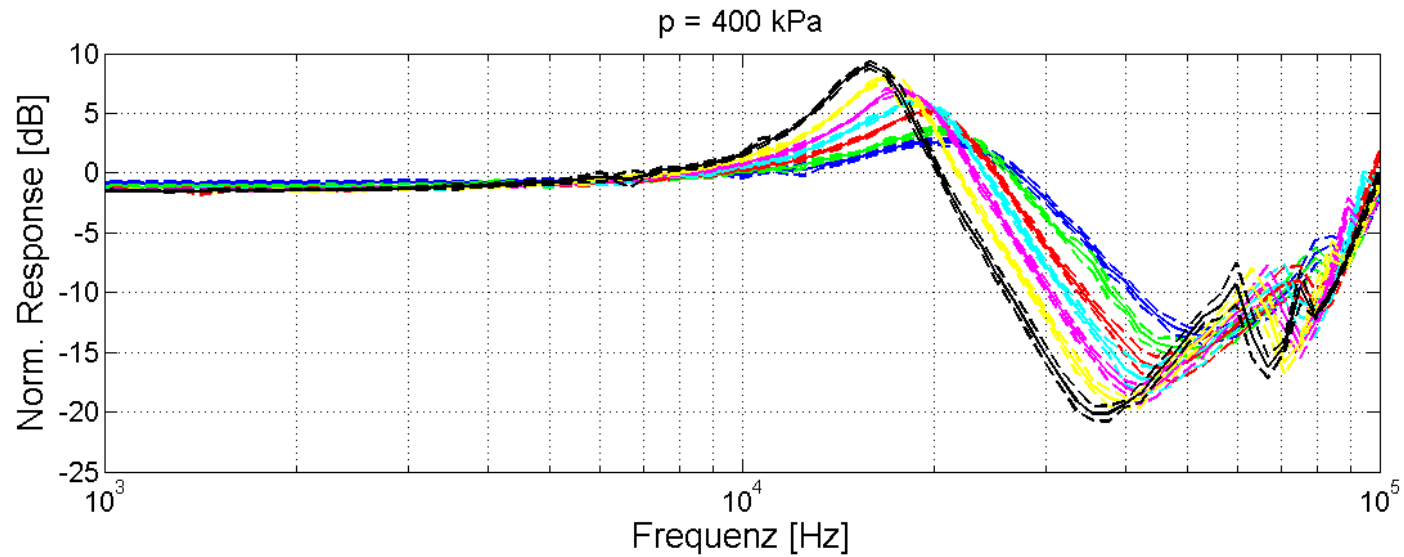
Spehr C. and Ahlefeldt T., "Comparison of Microphone Array Measurements in the Closed Test Section of LSWT and ETW", *CEAS Journal*, accepted for publication (2018).

Comparability – PSF



Sensor calibration – amplitude response

$p_{stat} = 400 \text{ kPa}$
 $120 \text{ K} \leq T \leq 290 \text{ K}$



With standard deviation

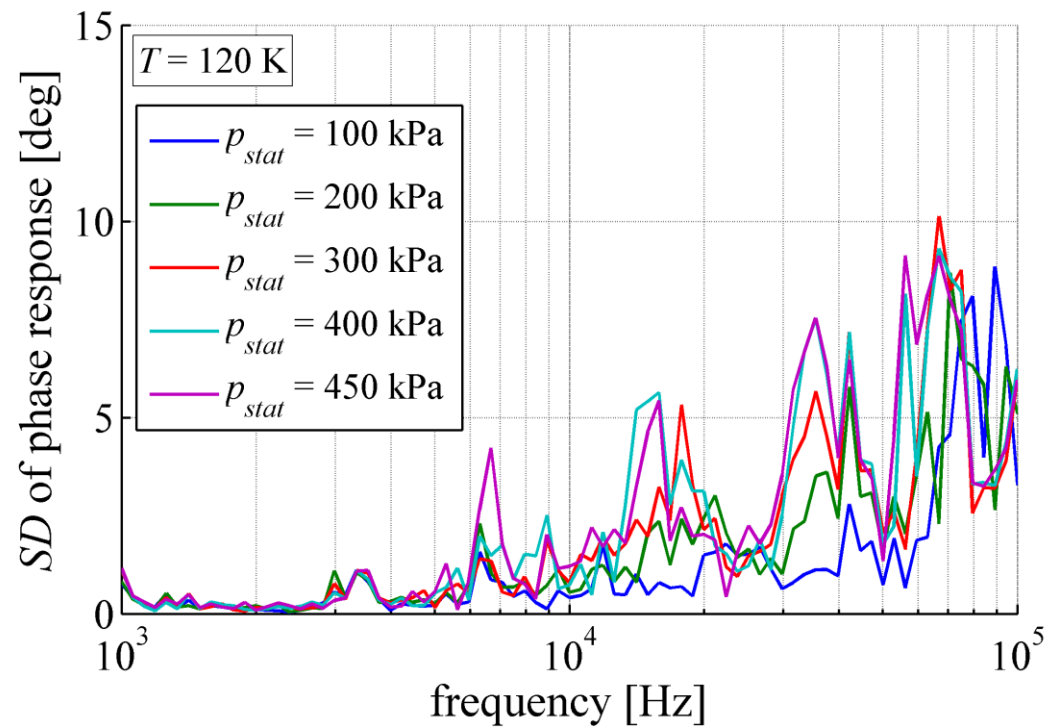


Sensor calibration – phase response

$T = 120\text{ K}$

$100\text{ kPa} \leq p_{stat} \leq 400\text{ kPa}$

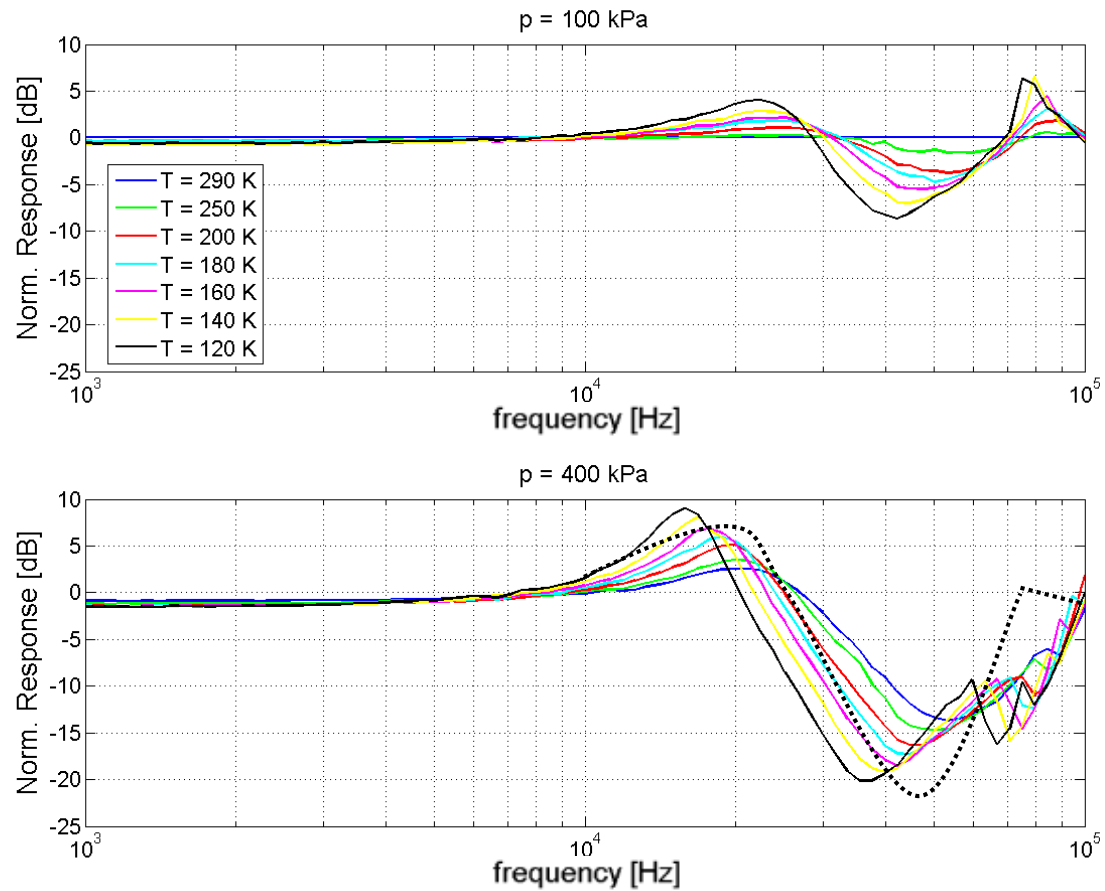
- Standard deviation up to 10 deg
- \approx commercially used array microphones
- Influence on beamforming result $< 0.05\text{ dB}$



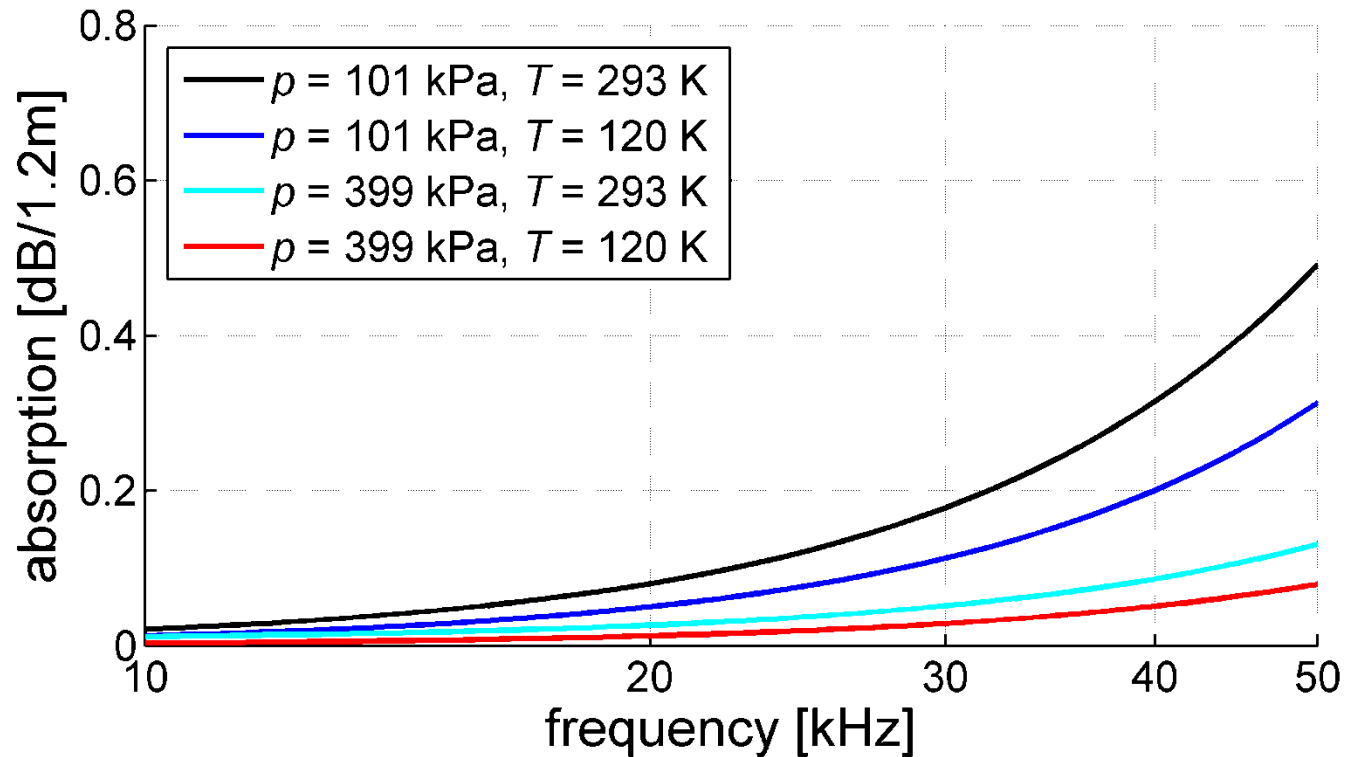
Ahlefeldt T., "Aeroacoustic Measurements of a Scaled Half-Model at High Reynolds Numbers", *AIAA Journal*, Vol. 55, No. 1 (2017).



Sensor calibration



Atmospheric absorption



- Shields, F. D.; Bass, H. E. “Atmospheric absorption of high frequency noise and application to fractional-octave bands” NASA CR-2760, 1977



$$\begin{aligned} M &= u/c \\ St &= fD/u \\ He &= 2\pi fD/c \end{aligned}$$

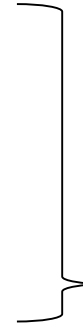
Assumptions / Corrections

- Aeroacoustic similarity:
Reynolds number, Mach number, Strouhal number, (Helmholtz number)

Test section environment

Static pressure p_{stat}

Temperature T



$$M = u/c$$

$$St = fD/u$$

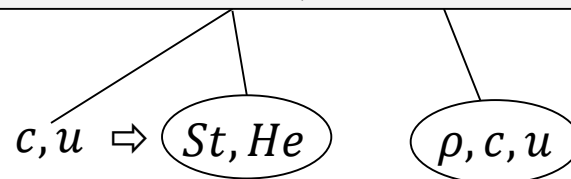
$$He = 2\pi fD/c$$

Assumptions / Corrections

- Aeroacoustic similarity:
Reynolds number, Mach number, Strouhal number, (Helmholtz number)

Test section environment	Changing properties	$M = \frac{u}{c} = \text{const.}$
Static pressure p_{stat}	Reynolds number	Reynolds number
Temperature T	density ρ	density ρ
	speed of sound c	speed of sound c
	Young's modulus E	\Rightarrow flow speed u \Rightarrow elastic deformation q/E

Source mechanisms: $p = \text{function}(\text{frequency}, \text{amplitude}, \text{Reynolds number})$



Results – Source maps (CLEAN-SC)

$M = 0.203$ | $\alpha = 3^\circ$ | *Variation of Strouhal number*

- Different Reynolds number
- 7% to **26%** of real-flight Re_δ
- Same deformation

$$Re_\delta = 1.42 \cdot 10^6$$

$$q/E = 1.57 \cdot 10^{-8}$$

$$Re_\delta = 5.16 \cdot 10^6$$

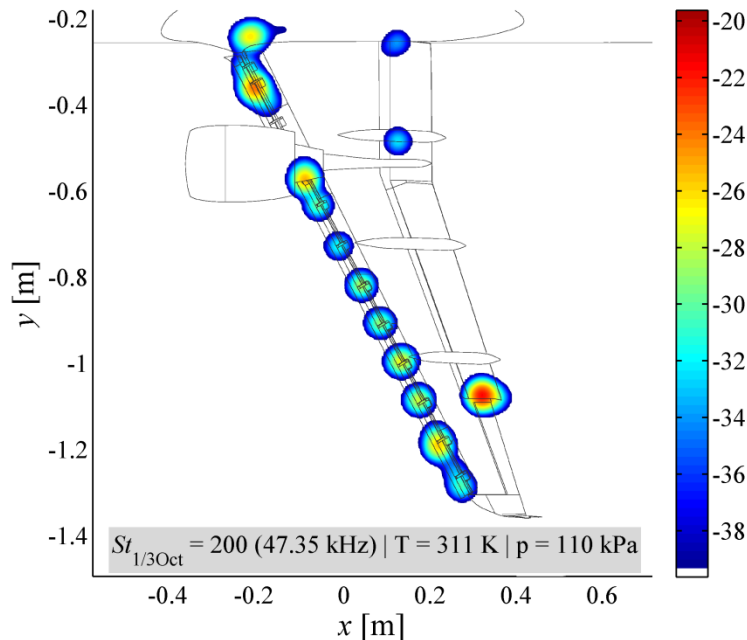
$$q/E = 1.57 \cdot 10^{-8}$$



Results – Source maps (CLEAN-SC)

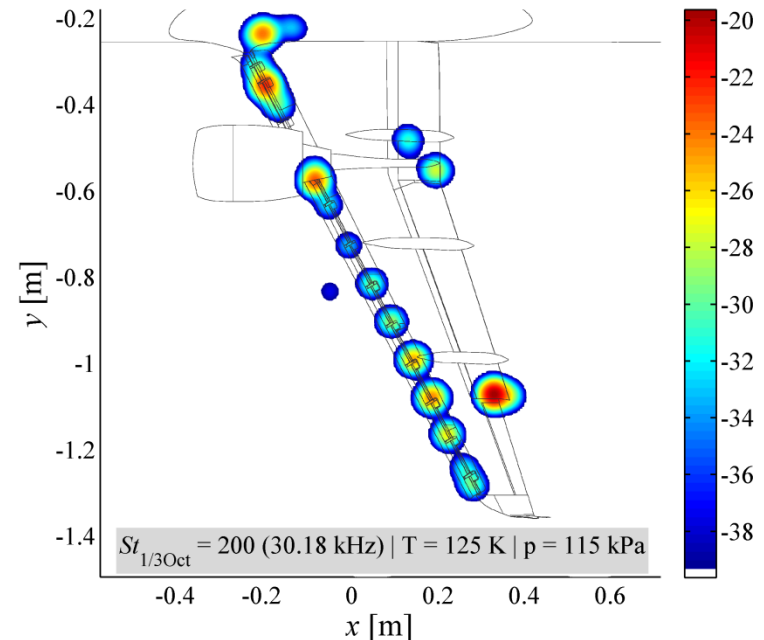
$M = 0.203 \mid \alpha = 3^\circ \mid$ Variation of Strouhal number

$$St_{\delta, 1300ct} = 200 \parallel f_{full-scale} = 335 \text{ kHz}$$



$$Re_\delta = 1.42 \cdot 10^6$$

$$q/E = 1.57 \cdot 10^{-8}$$



$$Re_\delta = 5.16 \cdot 10^6$$

$$q/E = 1.57 \cdot 10^{-8}$$



Results – Source maps (CLEAN-SC)

$M = 0.203$ | $\alpha = 3^\circ$ | *Variation of Strouhal number*

- Same Reynolds number
- **26%** of real-flight Re_δ
- Different deformation

$$Re_\delta = 5.16 \cdot 10^6$$

$$q/E = 1.57 \cdot 10^{-8}$$

$$Re_\delta = 5.16 \cdot 10^6$$

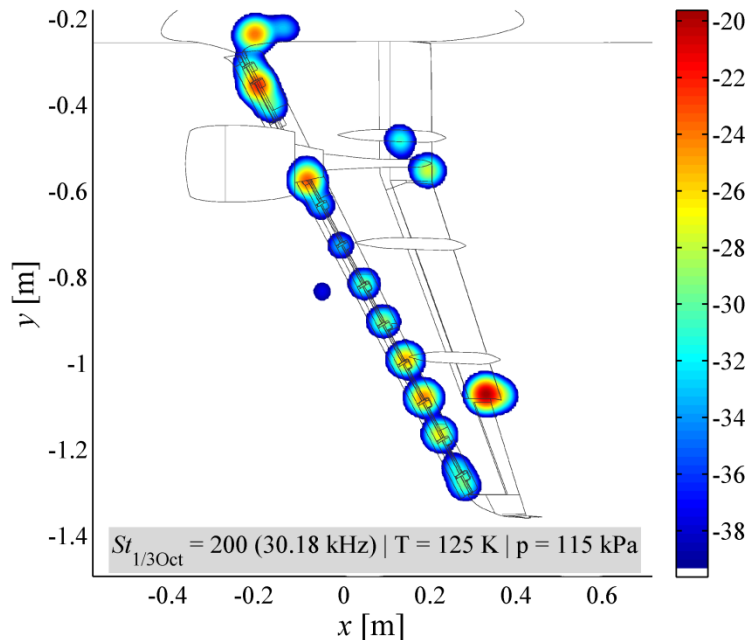
$$q/E = 5.70 \cdot 10^{-8}$$



Results – Source maps (CLEAN-SC)

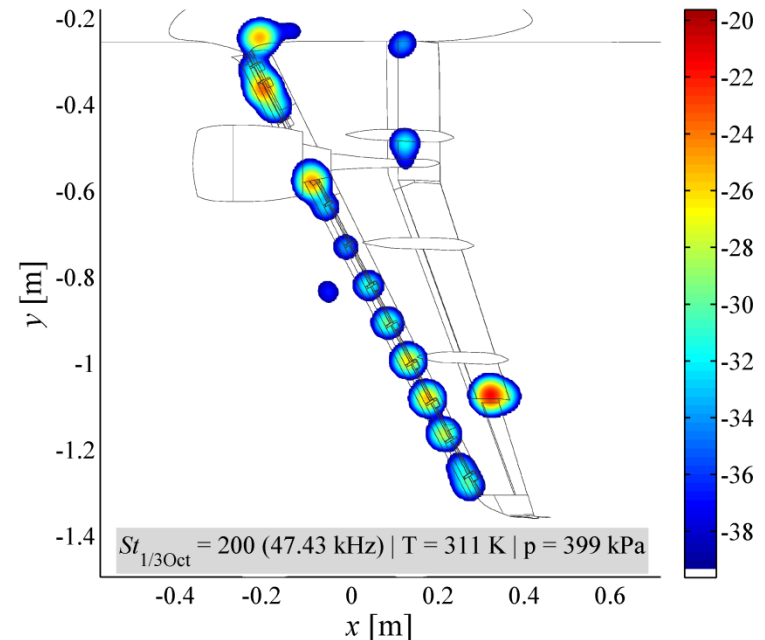
$M = 0.203 \mid \alpha = 3^\circ \mid$ Variation of Strouhal number

$$St_{\delta, 1300ct} = 200 \parallel f_{full-scale} = 335 \text{ kHz}$$



$$Re_\delta = 5.16 \cdot 10^6$$

$$q/E = 1.57 \cdot 10^{-8}$$



$$Re_\delta = 5.16 \cdot 10^6$$

$$q/E = 5.70 \cdot 10^{-8}$$



Results – Source maps (CLEAN-SC)

$M = 0.203$ | $\alpha = 3^\circ$ | *Variation of Strouhal number*

- Different Reynolds number
- **26%** to **100%** of real-flight Re_δ
- Same deformation

$$Re_\delta = 5.16 \cdot 10^6$$

$$q/E = 5.70 \cdot 10^{-8}$$

$$Re_\delta = 20.0 \cdot 10^6$$

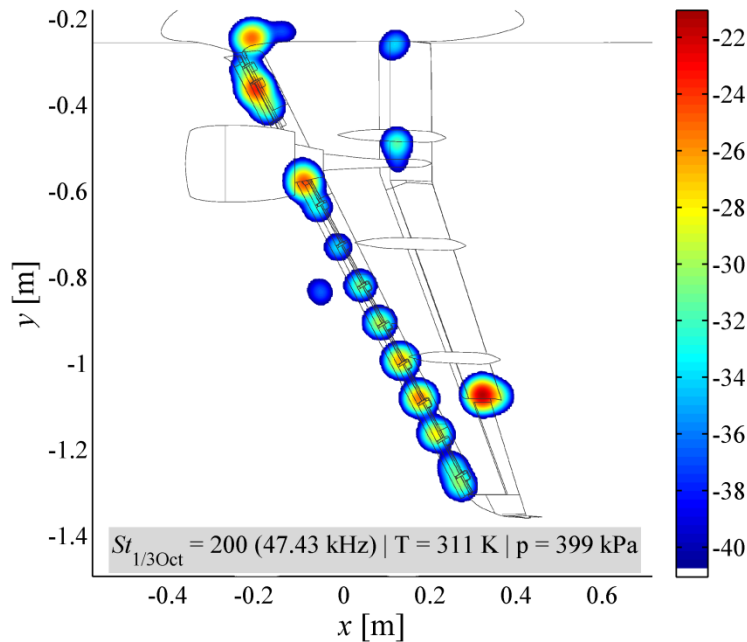
$$q/E = 5.70 \cdot 10^{-8}$$



Results – Source maps (CLEAN-SC)

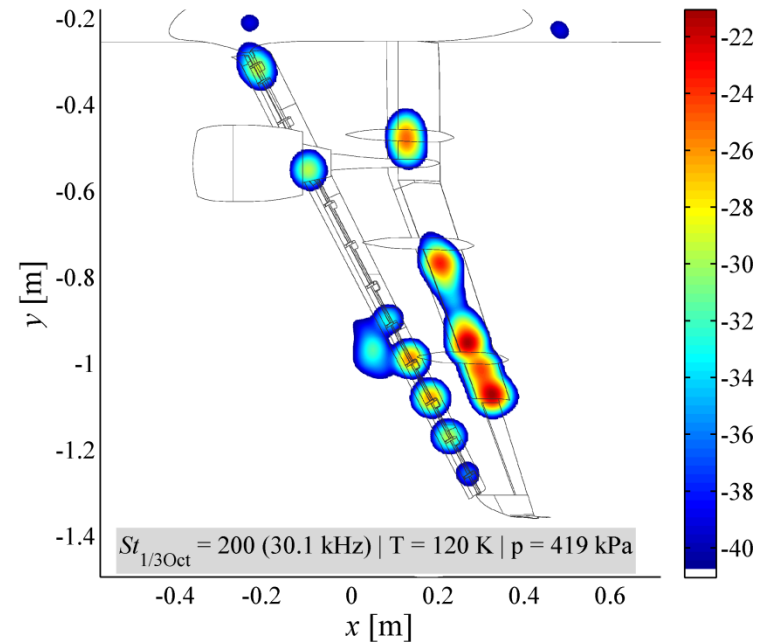
$M = 0.203 \mid \alpha = 3^\circ \mid$ Variation of Strouhal number

$$St_{\delta, 1300ct} = 200 \parallel f_{full-scale} = 335 \text{ kHz}$$



$$Re_\delta = 5.16 \cdot 10^6$$

$$q/E = 5.70 \cdot 10^{-8}$$

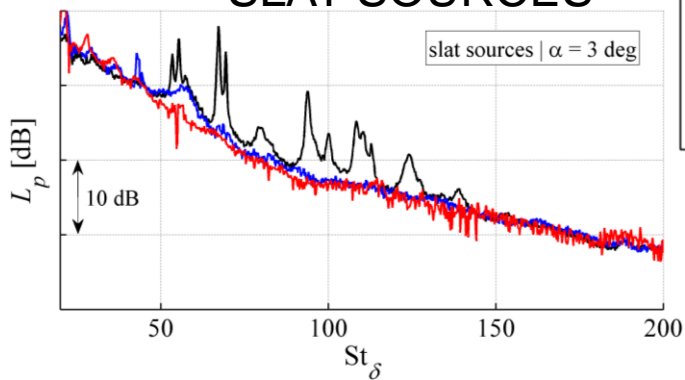


$$Re_\delta = 20.0 \cdot 10^6$$

$$q/E = 5.70 \cdot 10^{-8}$$

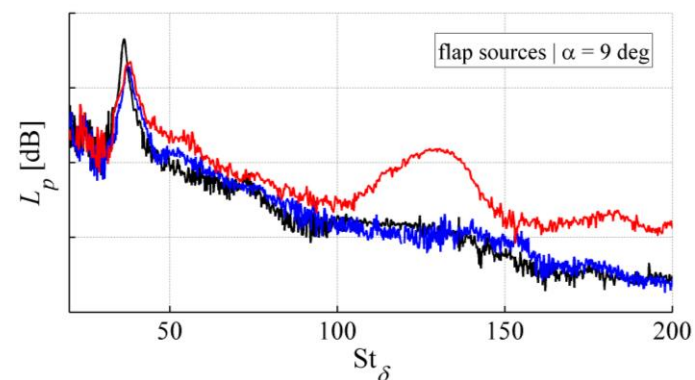
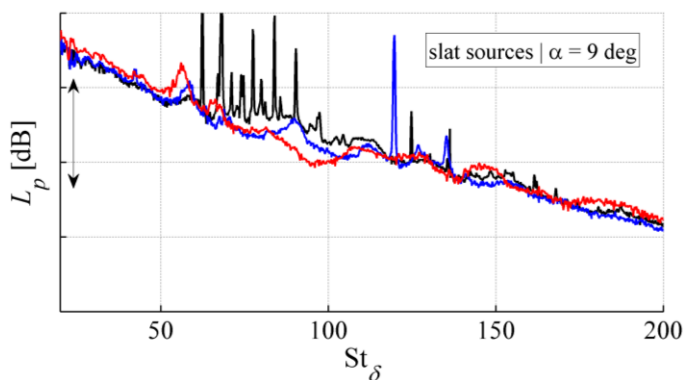
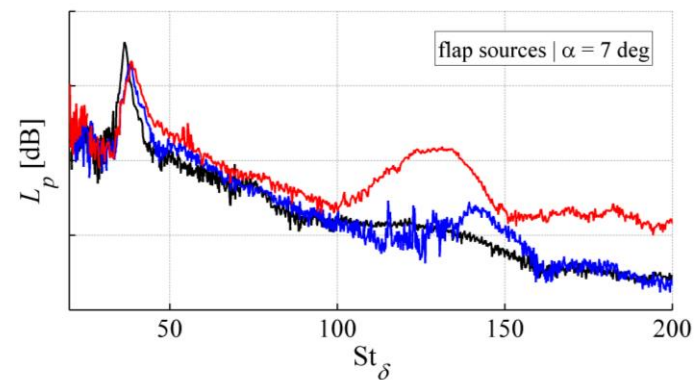
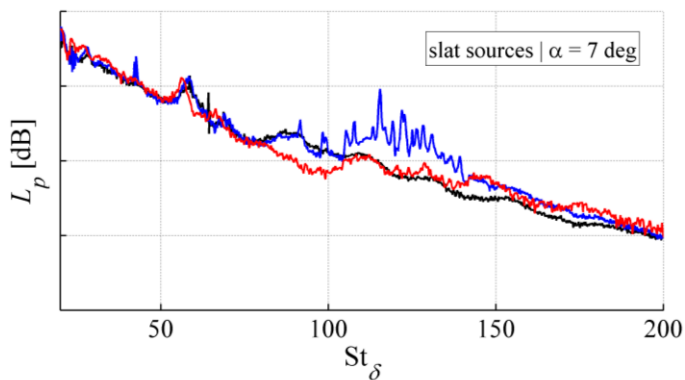
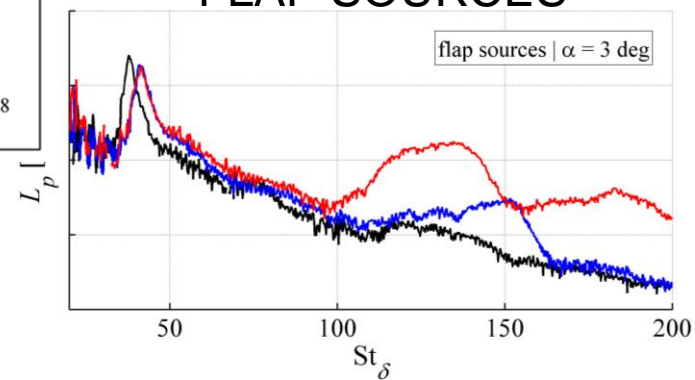


SLAT SOURCES



— DP I: $Re_\delta = 1.43 \cdot 10^6$ | $q/E = 1.55 \cdot 10^{-8}$
 — DP III: $Re_\delta = 5.17 \cdot 10^6$ | $q/E = 5.64 \cdot 10^{-8}$
 — DP IV: $Re_\delta = 20.06 \cdot 10^6$ | $q/E = 5.64 \cdot 10^{-8}$

FLAP SOURCES



Equations

$$\rho = \frac{p}{\mathcal{R}T} \quad (\text{ideal gas})$$

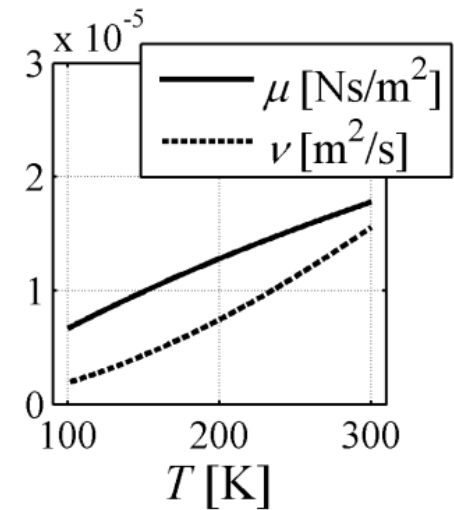
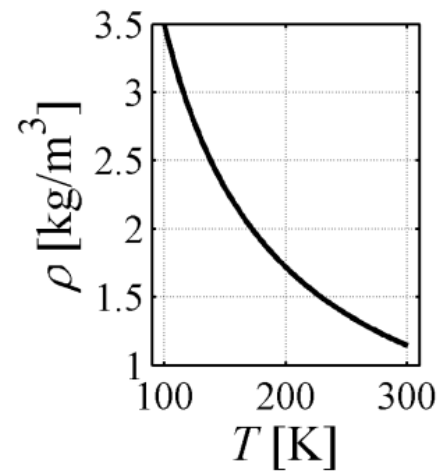
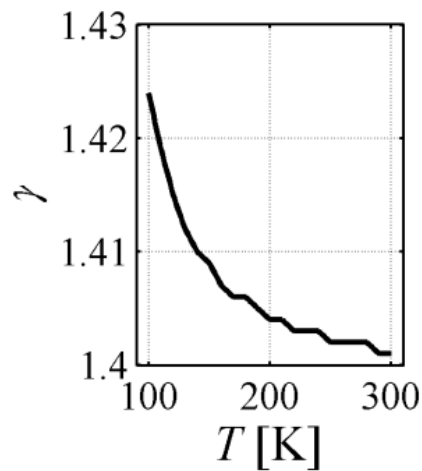
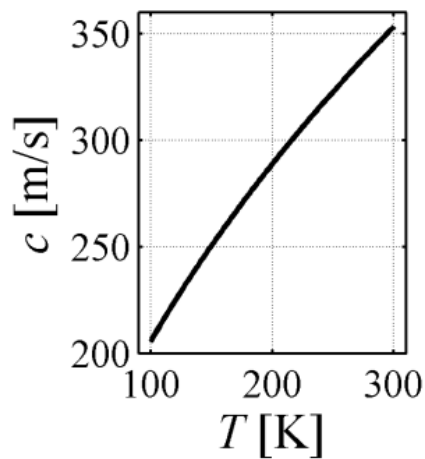
$$M = u/c$$

$$St = fD/u$$

$$He = 2\pi fD/c$$

$$c = \sqrt{\frac{\gamma(p, T)\mathcal{R}T}{m_{mol}}}$$

$$Re = \frac{\rho \cdot u_{\infty} \cdot d}{\eta} = \frac{\rho \cdot M \cdot d}{c \cdot \eta}$$



Electrostatic Actuator

$$P_{dynamic}[rms] = \frac{\epsilon \cdot E_0 \cdot e_{rms}}{d^2} \cdot R_{area}$$

$$\epsilon = \epsilon_r \epsilon_0$$

$$\epsilon_0 \approx 8.85 \cdot 10^{-12} \text{ F/m}$$

$$\epsilon_r(295 \text{ K}, 1.0 \text{ kPa}) \approx 1.0005$$

$$\epsilon_r(120 \text{ K}, 4.5 \text{ kPa}) \approx 1.0055$$

$$\Rightarrow \Delta dB \approx 0.04 \text{ dB}$$

where: E_0 = applied DC-voltage
 e_{rms} = rms value of applied AC-voltage
 $P_{dynamic}$ = produced dynamic pressure
 d = plate distance
 ϵ = dielectric constant of the gas between plates

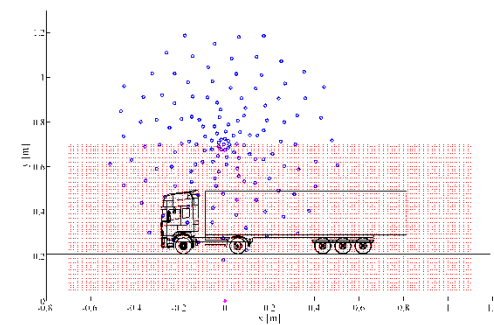
[*Microphone Handbook, Vol.1: Theory*, Brüel&Kjaer, July 1996, BE 1447-11]



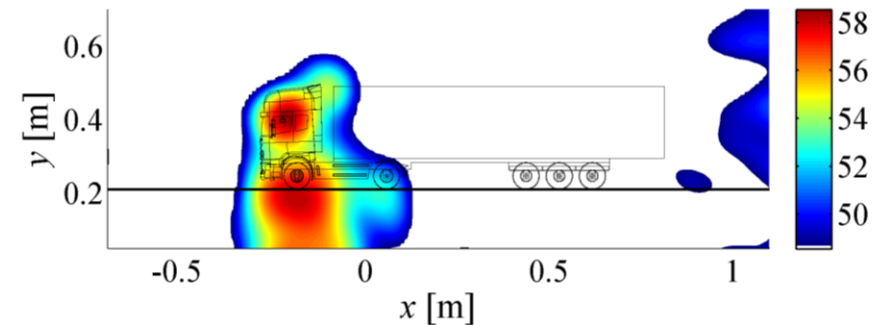
Repeat without disturbing sources

Source map $u = 40$ m/s; $\alpha = 0^\circ$

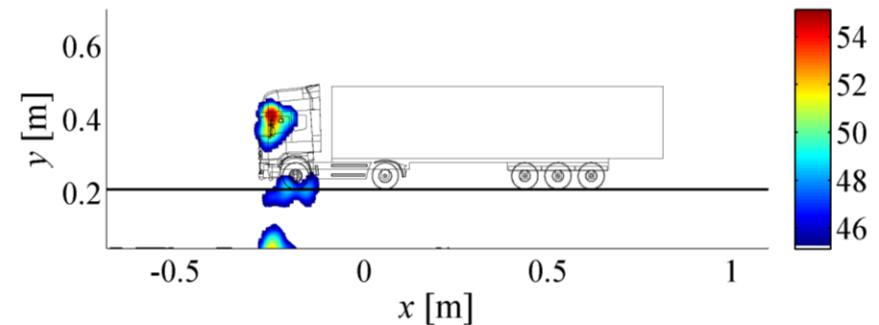
- Overview



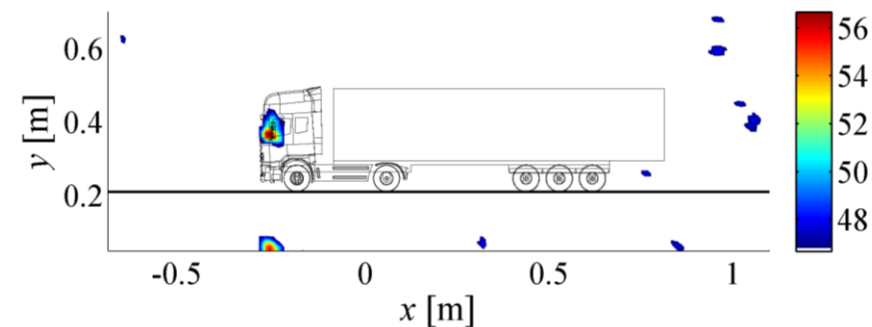
$f_{1/3\text{Oct}} = 5$ kHz



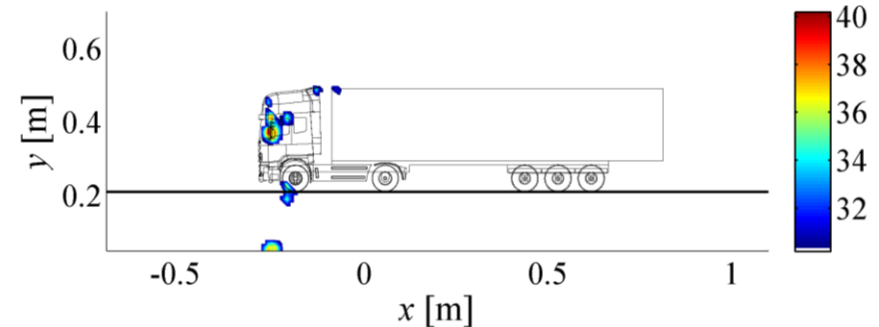
$f_{1/3\text{Oct}} = 16$ kHz



$f_{1/3\text{Oct}} = 25$ kHz

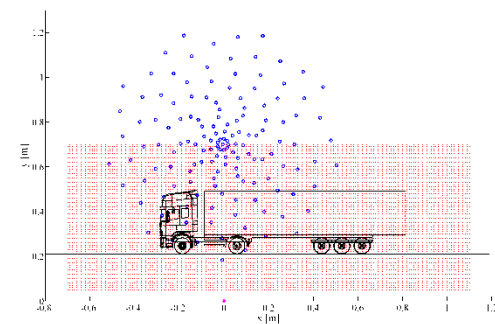


$f_{1/3\text{Oct}} = 50$ kHz



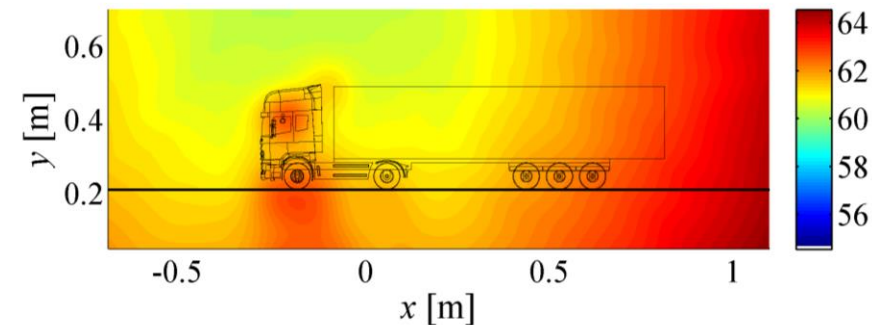
Repeat without disturbing sources

Source map $u = 40$ m/s; $\alpha = 0^\circ$

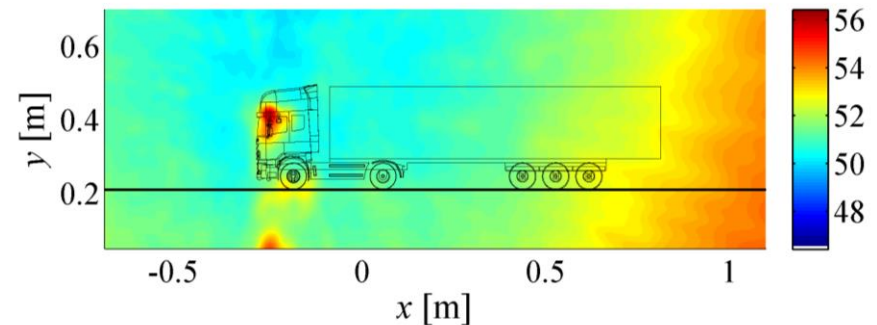


- Comparison: „Diagonal Removal off“

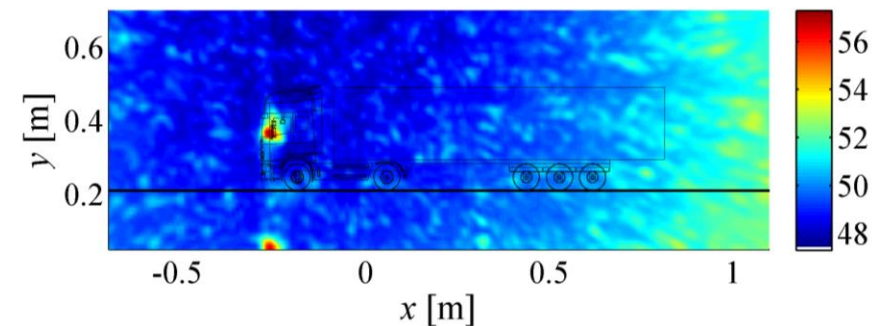
$f_{1/3\text{Oct}} = 5$ kHz



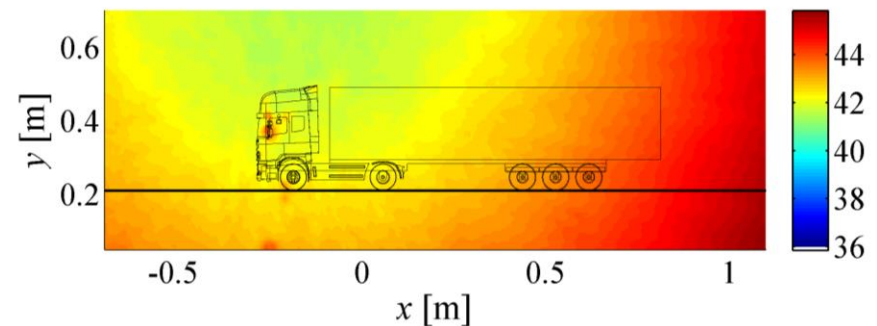
$f_{1/3\text{Oct}} = 16$ kHz



$f_{1/3\text{Oct}} = 25$ kHz



$f_{1/3\text{Oct}} = 50$ kHz



Interpretation of data

